Chemical composition/pharmacophore modelling-based, virtual screening, molecular docking and dynamic simulation studies for the discovery of novel superoxide dismutase (*SODs*) of bioactive molecules from aerial parts of *Inula Montana* as antioxydant's agents

Radja Achiri, Mesli Fouzia, Fatima Zohra Benomari, Nassim Djabou, Tabti Boufeldja, Alain Muselli & Mohammed El Amine Dib

Taylor & Francis
Taylor & Francis Group

Check for updates

Chemical composition/pharmacophore modelling- based, virtual screening, molecular docking and dynamic simulation studies for the discovery of novel superoxide dismutase (*SODs*) of bioactive molecules from aerial parts of *Inula Montana* as antioxydant's agents

Radja Achiri[a], Mesli Fouzia[a], Fatima Zohra Benomari[c], Nassim Djabou[c] (ID), Tabti Boufeldja[a], Alain Muselli[b] and Mohammed El Amine Dib[a]

[a]Laboratoire des Substances Naturelles & Bioactives (LASNABIO), Département de Chimie, Faculté des Sciences, Université Abou BekrBelkaıd, Tlemcen, Algeria; [b]Laboratoire Chimie des Produits Naturels, Université de Corse, UMR CNRS 6134, Corté, France; [c]Laboratoire de Chimie Organique, Substances Naturelles et Analyses (COSNA), Faculte des Sciences, Universite Abou BekrBelkaıd, Tlemcen, Algeria

Communicated by Ramaswamy H. Sarma

ABSTRACT

The accumulation of free radicals in the body develops chronic and degenerative diseases such as cancer, autoimmune diseases, rheumatoid arthritis, cardiovascular and neurodegenerative diseases. The first aim of this work was to study the chemical composition of *Inula Montana* essential oil using GC-FID and GC/MS analysis and the antioxidant activities using radical scavenging (DPPH) and the Ferric-Reducing Antioxidant Power (FRAP) tests. The second aim was to describe the assess the antioxidant activity and computational study of Superoxide Dismutase (SODs) and ctDNA inhibition. Sixty-nine compounds were identified in the essential oil of the aerial part of *Inula montana*. Shyobunol and α-Cadinol were the major compounds in the essential oil. The antioxidant power of the essential oil showed an important antioxidant effect compared to ascorbic acid and the methionine co-crystallized inhibitor. The results of the docking simulation revealed that E, E-Farnesyl acetate has an affinity to interact with binding models and the antioxidant activities of the ctDNA sequence and Superoxide Dismutase target. The penetration through the Blood-Brain Barrier came out to be best for E, E-Farnesyl acetate and E-Nerolidolacetate and was significantly higher than the control molecule and Lref. Finally, the application of ADMET filters gives us positive information on the compound E, E-Farnesyl acetate, which appears as a new inhibitor potentially more active towards ctDNA and *SODs* target. The active compounds, E,E-Farnesyl acetate can be used as templates for further development of more potent antioxidative agents.

1. Introduction

Highly reactive free radicals and oxygen species are present in biological systems from a wide variety of sources such the regular metabolism or external sources (Navidpour et al., 2007; Suthakaran et al., 2008). The action of free radicals is counteracted by free radicals endogenous or exogenous or synthetic route. Reactive oxygen species (ROS) such as superoxide anions, hydrogen peroxide, hydroxyl, and nitric oxide radicals, play an important role in oxidative stress related to the pathogenesis of various important diseases. The antioxidants are entities present at low concentration compared to that of oxidizable substrates (Halliwell, 1995). And which have the capacity to react with free radicals in order to delay or inhibit the oxidation of biological substrates, in other words, rendering them harmless (Al-Mamary et al., 2002). They have two origins, one endogenous represented by enzymes, and the other provided by food. On the other hand, synthetic antioxidants commonly used in pharmacological and food applications are phenolic compounds such as butylhydroxytoluene (BHT) and butylhydroxyanisole (BHA). However, following doubts about their carcinogenic and toxic effects, the latter were limited by legislative rules (Wichi, 1988). As a result, the interest that has been focused on identifying natural and safe alternative sources of natural antioxidants has continued to grow in recent years (Kabouche, 2014). Essential oils are a potential source of natural and bioactive molecules because their components have antioxidant power, and which could then be used as food preservatives to limit food spoilage. The *Asteraceae* family, also known by its compounds, is one of the most widely distributed in the plant kingdom and is particularly represented in temperate and cold regions of the globe. The latter has more than 13 tribes divided into 23,000 species and 1,500 genera whose Algerian soil includes 109 genera divided into 408 species, many of which are rich in producers of essential oils with biological properties (Adewole, 2002). The genus of *Inula* is among those

belonging to the family of compounds and which holds a variety of about 90 abandoned species distributed in the Mediterranean basin (Kabouche, 2014). Traditional medicine has granted multiple therapeutic properties to species of the genus of *Inula* . Including the species that was the subject of our study *I. montana* which has an activity on the digestive system (Pascual & Morales, 2002). So, in order to identify possible sources of this plant and in the context of researching new bioactive substances, our study is based on the determination of the chemical composition of the essential oil of *I. montana* gathered in the north-west of Algeria using GC-FID and GC/MS analyzes as well as the evaluation of its antioxidant activity.

The main interest was to develop unique potential inhibitors of the Superoxide Dismutase and ctDNA interaction, to combat free radicals and protect the body from the damage caused by them. Additionally, Modeling and simulation techniques are becoming an important research method for investigating operational and organizational systems and in particular in Chemistry. They are often necessary when the real experience is too difficult, too dangerous and too expensive. Digital chemistry subsidizes a better understanding of the action of medicinal plants against diseases and offers high-level training, focused on the study of living things at the molecular level. In addition, represents a bridge between theory and experience. It makes it possible to represent, interpret and predict biomolecular structures and functions (Nadia et al., 2020, Fouzia et al., 2018). However, there are no reports on chemical composition and biological activities of *I. montana* . Therefore, this work was aimed to study for the first time, the chemical composition of *Aerial* parts and the intraspecies variations of essential oils from 7 locations using statistical analysis and the second study was to try to test the molecules of this oil for their antioxidant activity by interested at the interaction with binding models and the antioxidant activities of the ctDNA and Superoxide Dismutase target. It is an important antioxidant, active in endothelial cells, cytoplasm and mitochondrial intermembrane matrix (Oury et al., 1996). SOD protects cells against superoxide damage through catalyzing the dismutation of superoxide radicals into molecular oxygen and hydrogen peroxide (Marikovsky et al., 2003; Oury et al., 1996) and thus inhibits peroxynitrite-mediated oxidative protein modification and cell membrane lipid peroxidation (Ischiropoulos et al., 1992).

On the other hand, we noted that in the last few years, the field of computer aided drug design and discovery (CADDD) by using different methods such as: molecular docking, molecular dynamics and ADME prediction is a rapid wing area that has seen many successes to discover and develop new drugs in medicinal chemistry.

The inhibition of Superoxide Dismutase was theoretically investigated by two methods of computational chemistry: molecular docking analyzes and molecular dynamics simulations. In this contribution, a combined of two theoretical approaches by using drug likeness, pharmacokinetics, medicinal Chemistry and ADME Properties to explore potential inhibitors among compounds of essential oils of Aerial parts

of *I. montana* against enzyme: Superoxide Dismutase and ctDNA. The docking studies predicted that the constituent molecules of Aerial parts of *I. montana* possess more capability as inhibitors as compared to established drugs in the pharmaceutical industry.

2. Material and methods

2.1. Expiremental procedures

2.1.1. Plant material and isolation of the essential oil
The aerial parts of *I. montana* were harvested at the flowering stage on May 2019 from 7 stations in Tlemcen (Algeria). The identification of the collected species was made by the laboratory of ecology and ecosystem management of the University of Tlemcen. The hydrodistillation of essential oils was done in a Clevenger type device for 5 h. The information of the habitats of the samples (places of harvest, altitudes and yield) is shown in (Table 1).

2.1.2. Identification of the oil components
2.1.2.1. Gas chromatography.
The analyzes by gas chromatography (GC) were carried out using a Perkin Elmer Clarus 600 chromatograph (Walton, MA, United States), equipped with a Split/Splitless injector, two capillary columns in fused silica (60 mx 0.22 mm ID, film thickness 0.25 μm), Rtx-1 (polydimethylsiloxane) and Rtx-Wax (polyethylene glycol). Also equipped with a double flame ionization detection injector.The programming of the oven temperature consists of an increase from 60° C to 230° C at 2° C/min, then in a plateau of 35 min at 230° C. The essential oils were injected in split mode 1/50.With a volume of 0.2 μL using hydrogen as carrier gas (0.7 ml min-1). The pressure at the top of the column was 25 psi with a flow rate of 1 ml/min.

2.1.2.2. Gas chromatography/mass spectrometry.
The samples were analyzed using a Perkin Elmer Autosystem XL chromatograph (Walton, MA, United States), equipped with an automatic injector and two columns (60 mx 0.22 mm ID, phase film thickness 0.25 μm stationary), polar (Rtx-Wax) and non-polar (Rtx-1).Coupled with a Perkin Elmer Turbo Mass mass detector. The temperature of the ion source is 150° C, the ionization energy is 70 ev. The injection was made via split mode with a division ratio of 1/80. Mass spectra were acquired over the 35-350 Da mass range. And for the chromatographic conditions (temperature programming, carrier gas, etc.) are the same as those described above.

2.1.2.3. Component identification and quantification.
The components were identified (i) by comparing their GC retention indices (RI) on non-polar and polar columns with those of standard standards (laboratory library "Aroma") or those reported in the literature. (ii) as well as by computer correspondence with the commercial mass of spectral libraries (Jennings & Shibamoto, 1980; National Institute of Standards and Technology, 1999) and comparison of the spectra with those of the laboratory's internal library. The quantification of the constituents was carried out via a flame ionization

Table 1. Data relative to harvest locations of *I. montana* from Algeria.

Spieces	N°	Voucher codes	Localities	GPS coordinates	Yields	Alt
Inula montana	S1	IM-1020-I1	Sidi wchaa	35°06′55″N; 1°46′37″O	0,09	54
	S2	IM-1020-I2	Bouzedjar	35°34′42″N; 1°08′03″O	0,02	26
	S3	IM-1020-I3	Ouchba	34°54′00″N; 1°13′20″O	0,06	780
	S4	IM-1020-I4	Werdania	35°16′49″N; 1°30′13″O	0,18	107
	S5	IM-1020-I5	Ain fezza	34°52′26″N; 1°12′36″O	0,1	780
	S6	IM-1020-I6	Oued tafna	34°45′29″N; 1°34′04″O	0,09	772
	S7	IM-1020-I7	Oum el Alou	34°49′00″N ;1°16′15″O	0.01	1022

detector by internal normalization of the peak areas calculated by integrating the response factors FID relative to tridecane (0.7 g/100 g) used as internal standard (Djabou et al., 2013).

2.1.2.4. DPPH free radical scavenging assay.
The antioxidant power of the essential oil has been tested by the method that uses DPPH (2,2-Diphenyl Picryl-Hydrazyl). The reaction is carried out in a total volume of 100 µl of different concentrations included between [0.05-0.09]. Subsequently added to 25 µl of the methanolic solution of DPPH (0.5 mM) followed by incubation for 30 min in the dark and at room temperature. The absorbances were tested using a spectrophotometer at 517 nm. The same concentrations were prepared for ascorbic acid to serve as a positive control. The antioxidant activity is evaluated using the following equation:

$$AA\% = \frac{(Abscontrol - Abstest)}{Abscontrol} \times 100 \qquad \text{Eq. (1)}$$

Where: AA: antioxidant activity, Abs: absorbance. The IC_{50}'s was calculated graphically by the linear regression formula of the inhibition percentages as a function of different concentrations of the sample tested.

2.1.2.5. Ferric-Reducing antioxidant power assay.
The reducing power of iron (Fe^{3+}) was evaluated using the Oyaizu technique (Oyaizu, 1986).The different concentrations of the essential oil (from 0.5 to 50 mg/L) were mixed with 2.5 ml of the phosphate buffer solution (0.2 M, pH 6.6) and 2.5 ml of to 1% solution of potassium ferricyanide K3Fe (CN) 6. Then the whole was incubated for 20 min at 50 °C. Once the incubation was completed 2.5 mL of trichloroacetic acid (10%) was added in order to stop the reaction. The whole was centrifuged at 3000 revolutions for 10 min. We followed the same technique of (El Omari et al., 2019), at the end 2.5 ml of the supernatant was mixed with 2.5 ml of distilled water. Absorbances were measured at 700 nm using a double visible beam spectrophotometer against ethanol as blank. Ascorbic acid was used as a positive control. The analyzes were carried out in triplicate.

2.2. Theoretical background and comptional details

2.2.1. Preparation and optimization of both enzyme and inhibitors
In this study, the structures of all inhibitors were downloaded from the PubChem database (https://pubchem.ncbi.nlm.nih.gov) (Wang et al., 2017) and CHEMBL database

(https://www.ebi.ac.uk/chembl) The PDB database (https://www.rcsb.org/) was worm to obtain the complete structure of Superoxide Dismutase (PDB ID: **2wz5** (Antonyuk et al., 2010). In general, the protein structure with a resolution between 1.5 and 2.5 Å have an excellent quality for further studies (Clément & Slenzka, 2006; Didierjean & Tête-Favier, 2016), whereas, the resolution value of Superoxide Dismutase and B-DNA belongs to this interval. The 3 D structures of Superoxide Dismutase enzyme and B-DNA sequence were obtained by X-ray diffraction with resolution 1.50 Å, 1.90 Å and R-Value Free 0.255, 0.178 respectively (Fig.1). The RMSD obtained by molecular docking varies between 0.116 and 1.154 according to table 5; the ligands tested are superimposed by the addition of the reference ligand (co-crystallized), which proves the correct choice of the enzyme. In addition, the structure of the co-crystal (reference ligand) of this SOD1 enzyme resembles the molecules of our plant.

Amyotrophic lateral sclerosis (ALS) is the most common degenerative disease of motor neurons in adults and has also been shown to be a type of conformational disease associated with improper folding and dysfunction of proteins.

- To date, over 150 distinct genes have been shown to be associated with ALS, of which *Superoxide Dismutase 1 (SOD1)* is the first and most studied and is classified as mutant human SOD1 (Huai & Zhang, 2019). It has been well established that the toxicity mediated by SOD1 mutants is caused by gain in function rather than loss of the detoxifying activity of SOD1.

A large body of evidence has shown that SOD1 mutants can adopt a complex conformation profile and interact with a wide range of client proteins.

The Protein data bank (PDB) format of ligand and complexes was obtained from Chemdraw (MM2) energy minimized file and by converting its file using the Mercury software. The crystal data of the B-DNA dodecamer d (CGCGAATTCGCG)$_2$ (PDB ID: **1BNA**) (Drew et al., 1981) were downloaded from the Protein Data Bank. The water molecules were removed from the 1BNA using MOE before performing docking calculations.

2.2.2. Molecular docking
Molecular docking is a structure-based drug designing approach used to find out the best orientation and key interactions between ligand and receptor. Molecular docking simulation was performed on the X-ray crystal structures of Superoxide Dismutase (PDB code: **2wz5**) and B-DNA
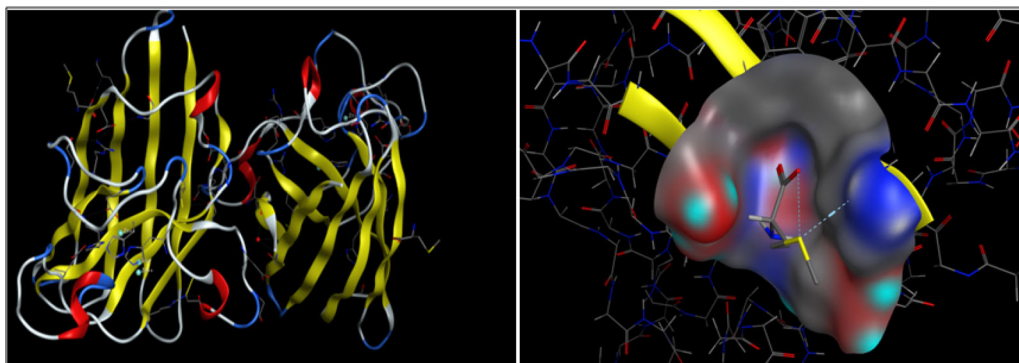
Figure 1. Enzymatic cavity with the residues of the active site for the target: **2wz5** detected by site finder (MOE).

sequence utilizing Molecular Operating Environment (MOE) software.

In this study, the software package MOE (Molecular Operating Environment) was introduced to study the modeling applications between essential oils of *Aerial parts of l. montana* compounds and the Superoxide Dismutase enzyme. MOE runs on Microsoft windows, mac Os and Linux (Molecular Operating Environment (MOE), 2013). The wash setting was applied at pH 6.0 and 300 K, hydrogen atoms were added, and protonation 3 D was assigned. The minimum energy configuration was performed using the MMFF94x force field. OPLS-AA force field was used (Jorgensen et al., 1996).To assign atom type and partial charges in receptor structure. The number of interactions varies between (0, n) where n is 10, the *cut-off* for coulomb interaction *and Vander Waal* interaction was 30 Å with the ability to study the hydrogen-electrostatic in the total active site of Superoxide Dismutase was optimized and the results were discussed. The predicted orientations and binding modes of essential oils of Aerial parts of *l.montana* compounds into the target Superoxide Dismutase were then visualized using software package MOE. For molecular docking calculations, we followed the same steps (same protocol) used in our previous studies (Chenafa et al., 2021; Daoud et al., 2018) and the default parameters are: Placement: Triangle Matcher; Rescoring 1: London dG (the scoring function was employed to estimate the lowest free energy of the complex with the best pose of ligand tested). During the docking process the ligand was considered structurally rigid while the target was set as completely flexible. At first, we minimized the energy of the enzymes and the ligands and their geometries were conducted using Hamiltonian AM1 implanted in MOE software and then isolation of the active site of the targets was carried out. The most stable conformation of each compound was minimized by the *same* semi-empirical method (*A*M1) (Stewart, 2007). All simulations were run by using all explicit solvation models using TIP3P water. (Semaoui et al., 2020) After that, the RMSD value was used to compare the differences between the atomic distances of the docked poses and the ligand molecule of reference pose, where a threshold of 2.0 Å corresponding to better solutions (Cross et al., 2009). In the end, positioning the ligands into the enzyme's active site was done using the docking module implanted in MOE software and, the binding energy (score) between ligands and targets was calculated using molecular mechanics (Molecular

Operating Environment (MOE), 2013) and based on molecular mechanics (Halgren, 1996; 1999). The results of the top-scoring docking poses were constructed and the best scoring complexes in the active site were selected for the further MD simulation study (Dal Ben et al., 2013).

2.2.3. Molecular dynamics simulation, ADMET, PASS cytochromes P450 and pharmacophore mapping

The top compound which has high binding affinity (Score) and one almost a stable interaction) with the Superoxide Dismutase target was subjected to Molecular Dynamics Simulations. Molecular dynamics was run by NAMD for 20 − 100 ns achieved for both the complex (2wz5-ligand) was carried out through MOE software (Molecular Operating Environment (MOE), 2013). Dynamics simulation needs the following parameters: sample time: 1 and time step: 0.001 for running simulation. The Langevin equation (Toda et al., 1991) is used in NAMD to generate the Boltzmann distribution for (canonical NVT, isobar-isotherm NPT) units and simulations. The Brunger-Brooks-Karplus (BBK) method (Brünger et al., 1984) is used to integrate the Langevin equation. The stochastic equations of motion (position and velocity) are described by Fokker-Planck (Wang & Skeel, 2003). The detailed analysis of (MD) simulation results of complexe L69 with target Superoxide Dismutase is summarized in (See Figures 6 and .7). Moreover, the stable conformation obtained in the MD simulation between the best two ligands and Superoxide Dismutase target was conducted by iMODS. Internal coordinate's normal mode analysis server (IMODS) has been used for many years in online modeling of protein flexibility to investigate the values of deformability, eigenvalues, variance, co-variance map and elastic network. The software package MOE (Molecular Operating Environment) has proven its performance in several recent studies and has been invoked, for example in: Fouzia & Salim, (2019), Daoud et al., (2018), and Chenafa et al., (2021). That's why was used for our research. Among the 69 selected compounds the molecular structures of the best compounds were analyzed using a SWISSADME server (http://www.swissadme.ch/). The results of Absorption, Distribution, Metabolism and Excretion for selected compounds are listed in Table 11. These results prescribe that the ADMET-score would be a comprehensive index to estimate chemical drug-likeness. The drug score associate druglikeness, cLogP,logs, molecular weight and toxicity risks in one handy value than may be attuned to judge the compound's overall potential for

quality for a drug (Filimonov at al., 2014 & Geronikaki et al., 1999 and Lipinski et al., 1997). In this research, prediction and significant descriptors of druglikeness such as mutagenicity, toxicological dosage level for different tissues and pharmacologically relevant properties of the compounds were predicted using a PreADMET server (http://preadmet.bmdrc.org/) and admetSAR server (http://lmmd.ecust.edu.cn:8000/) (Cheng et al., 2012). The PASS (Prediction of Activity Spectra for Substances) may be efficiently used to find new targets for some ligands and, conversely, to reveal new ligands for some biological targets, and there are also many research where PASS predictions were approved by biological samples, subsequent synthesis and immunological analysis and cell test (Filimonov et al., 2014; Singh et al., 2014). The PASS predictions of the two best selected ligands were performed using the PASS-Way2Drug server. The results of the PASS prediction studies are summarized in Table12. Cytochromes P450 are key enzymes involved in the metabolism of various endogenous or exogenous molecules. The results of The P450 sites of metabolism (SOM) of the two best selected compounds were determined by online tool, RS-WebPredictor 1.0 (Release, 2018) and listed in (See Supplementary Materials Table S7). The process of deriving pharmacophore is known as pharmacophore mapping. The pharmacophore mapping study of the best ligands was carried out by online server PharmMapper. It consists to identify a common binding element that is responsible for the biological activity and determining the 3 D relationship between pharmacophore elements in each conformation generated. The pharmacophore mapping study of the two best ligands was carried out by online server PharmMapper (Parr, 1989). The pharmacophore modelling was done for the best ligand molecule among the 69 selected ligand molecules is summarized in Fig. 9. The conformations of the dataset were generated by using default settings in software MOE version 2013.08. MOE is comprehensive drug discovery software used ligand and structure-based pharmacophore modeling. However, in this study, we used ligand-based pharmacophore modeling to reveal the chemical features important for the compounds activity against IGF-1R. The Scientific Vector Language (SVL) command-line is provided by MOE that integrates with database browsers which helps in the formation of packed conformation dataset (Chen & Foloppe, 2008). The conformational search module in MOE was used to generate minimum energy conformations of each active and inactive compound.

A conformation training dataset of 20 chemical compounds was implemented in MOE to generate pharmacophore hypothesis. The dataset consisted of 20 active and 4 (α-Curcumene, Zingebrene, E, E-α-farnesene and trans-calamenene inactive compounds were employed to influence the quality of pharmacophore models depending on the two basic values are specificity and sensitivity. Active compounds have well known pharmacokinetics properties such as drug absorption, distribution, metabolism and excretion that directly bind to target receptors while inactive compounds had a poor binding affinity (Chen & Foloppe, 2008). In the present study, only active compounds were selected with common features such as HBDs, HBAs, Aro, HyD, number of nonpolar atoms and rotatable bonds. The developed

pharmacophore model was selected based on molecular sequence and low RMSD (see Table 5). However, the P450 sites of metabolism (SOM), Prediction of Activity Spectra for Substances, pharmacophore mapping, druglikeness prediction and ADMET- calculations were carried out to determine and compare the biological activities of the two best ligands.

3. Results and discussion

3.1. Experimental approach

3.1.1. Chemical composition of I.montana essential oils

The hydrodistillation of dry leaves of *I.montana* collected from seven different regions for 4 h has resulted in essential oils of yellowish color. The essential oil yields for each station are mentioned in Table 1. The essential oil yields vary from 0.01% to 0.18% (w/w), from one station to another. The highest essential oil yields were obtained in the stations of Wardania (0.18%) (S4) and Ain fezza (0.1%) (S5) with altitudes of 107 m to 780 m respectively, the stations of Sidi wchaa (S1) which is located at 54 m and Oued tafna (S6) which is located at 772 m posted the same yield which is in the order of (0.9%). For the station of Ouchba (S3) which is located at an altitude of 780 m, the yield was (0.06%). While the lowest yields were observed in the stations of Bouzadjar (0.02%) (S2) and oum el alou (0.01%) (S7) with altitudes varying from 26 m to 780 m.

The components of the essential oil were identified by comparing their mass spectra (EI-MS) and their retention indices (RI) with those of the mass spectra library (Table 2). The essential oil of *I. montana* demonstrated the predominance of sesquiterpene components (99.2%) from the identified content. The oxygenated sesquiterpenes were the most dominate with a percentage of 74.3%. The main ingredients were Shyobunol (19.2%), α-cadinol (12.2%), tau-Cadinol (6.7%), δ-Cadinene (8.2%), Veridiflorol (3.5%), Caryophyllene oxide (3.2%), Z, E-Farnesyl acetate (6.4%) and ar-Curcumen-15-al (3.4%) (Table 2). It should be noted that the essential oil of the aerial part of *I. montana* has never been studied before. However, the chemical composition of the essential oils of other *Inula* species has been widely studied; according to geographical and botanical origins of the samples, monoterpenes (p-Cymene, Thymol, Bornylacetate … etc) have been reported as the main component classes, but when we compare our results with those of other *Inula* species from different regions which were widely studied we notice a difference in the chemical composition, but the class of monoterpenes remains the predominant one (Table 13).

The major component of essential oil of leaves of *I. ensifolia* and *I. salicina* collected in Bulgaria (Trendafilova et al., 2020), and *I. verbascifolia* collected in Croatia (Giamperi et al.., 2010) consist mainly of hexadecanoic acid (8.1%, 8.3%, and 10.4%) respectively. While bornyl acetate was detected as the main constituent in essential oil of *I. oculus-christi* from Turkey (21.3%) (Kilic̦, 2014), in *I. viscosa* from Algeria (39.81%) (Boumaza, 2011) and *I. graveolens* from France (54%) (Boumaza, 2011).On the other hand, p-Cymene was detected as the main component of esseniatl oil of *I. crithmoides* collected in Tunisia (27.3%) (Jallali et al., 2014), Spain (53.8%) (Tsoukatou & Roussis, 1999), central Italy (30.1%)

Table 2. Chemical composition of the essential oil of leaves of *l. montana*.

No	Components	IRI$_a$[b]	Rl$_a$[c]	Rlp[d]	S1	S2	S3	S4	S5	S6	S7	Identification
1	Hexanal	773	770	1055	0,1	0,2	0,1	tr	tr	tr	0,2	RI, MS
2	Z-hex-3-en-1-ol	834	831	1380	0,2	tr	0,3	tr	tr	tr	0,5	RI, MS
3	β-citronelle	938	940	1031	tr	0,1	0,1	tr	0,1	tr	0,1	RI, MS
4	6-methyl-hept-5-en-2-one	961	963	1337	0,2	tr	tr	tr	tr	0,1	0,1	RI, MS
5	1,8-Dihydro cineole	979	979	1180	0,1	tr	0,3	0,1	0,6	0,1	0,4	RI, MS
6	Octanal	981	982	1169	0,2	0,1	0,2	0,1	0,5	0,1	0,2	RI, MS
7	Nonal	1082	1083	1394	0,1	0,1	tr	0,4	0,3	0,2	0,1	RI, MS
8	α-Terpineol	1179	1175	1688	0,2	tr	0,4	tr	0,1	0,1	0,1	RI, MS
9	Theaspirane 1	1293	1292	1480	0,1	tr	0,1	0,1	0,1	0,1	tr	RI, MS
10	cis-3-Hexenyl tiglate	1305	1304	1641	0,1	tr	0,1	0,1	0,1	0,1	0,1	RI, MS
11	Theaspirane 2	1308	1307	1517	0,1	tr	0,1	0,1	tr	0,1	0,1	RI, MS
12	α-Cubebene	1348	1350	1452	0,1	tr	0,1	0,2	tr	tr	0,1	RI, MS
13	α-Ylangene	1375	1372	1476	0,2	0,1	0,2	0,2	0,2	0,1	0,2	RI, MS
14	α-Copaene	1379	1379	1488	0,1	tr	0,2	0,1	tr	tr	0,2	RI, MS
15	β-Borbonene	1383	1385	1515	0,2	0,1	tr	0,3	0,2	0,1	0,1	RI, MS
16	Cyprene	1402	1406	1525	0,3	0,3	0,3	tr	tr	0,5	0,7	RI, MS
17	cis-α-Bergamotene	1409	1411	1562	0,3	tr	0,2	tr	0,1	tr	0,2	RI, MS
18	α-Ghurjunene	1413	1410	1524	0,2	0,4	0,4	0,9	0,9	1,1	1,6	RI, MS
19	Aristolene	1420	1416	1560	0,1	0,1	0,1	tr	0,1	tr	tr	RI, MS
20	E-β-Caryophyllene	1424	1418	1524	0,3	0,3	0,9	0,1	0,1	0,4	1	RI, MS
21	β-Copaene	1426	1431	1581	0,1	0,4	0,3	tr	0,2	tr	0,1	RI, MS
22	β-Ghurjunene	1439	1439	1591	0,3	0,2	0,2	0,1	0,2	0,2	0,3	RI, MS
23	E-β-Farnesene	1448	1448	1660	0,3	0,4	0,2	0,3	0,6	0,2	0,1	RI, MS
24	Nomadendrene	1452	1450	1581	0,2	tr	0,1	tr	0,1	tr	0,3	RI, MS
25	α-Humulene	1456	1451	1611	0,4	0,1	0,1	0,6	0,1	0,4	0,4	RI, MS
26	Allo-aromadendrene	1462	1463	1476	0,2	0,1	0,5	0,3	0,8	0,4	0,4	RI, MS
27	α-Curcumene	1471	1468	1465	0,2	0,1	0,6	0,3	0,3	0,1	0,4	RI, MS
28	γ-Muurolene	1471	1471	1681	0,2	0,1	0,3	0,5	0,3	0,5	1	RI, MS
29	Germacrene D	1480	1480	1704	0,3	0,5	0,6	1,1	1,8	0,3	0,1	RI, MS
30	Zingebrene	1486	1489	1717	0,1	0,2	0,1	0,3	tr	0,2	0,3	RI, MS
31	α-Muurolene	1496	1994	1719	0,3	0,1	1,5	1,1	2,7	0,2	1	RI, MS
32	E,E-α-Farnesene	1498	1500	1740	0,3	tr	tr	0,1	0,6	0,1	0,1	RI, MS
33	γ-Cadinene	1507	1507	1752	1	1,4	2,1	2,1	1,7	1,2	1	RI, MS
34	trans-Calamenene	1512	1511	1816	0,3	tr	0,5	0,9	0,5	0,5	0,3	RI, MS
35	δ-Cadinene	1516	1516	1752	9,7	9,2	7,7	8,4	8,9	5,1	3	RI, MS
36	α-Cadinene	1535	1530	1740	0,3	0,5	0,7	0,4	0,7	0,3	1,3	RI, MS
37	α-Calacorene	1531	1531	1895	1,1	0,2	0,5	0,4	0,7	0,2	1	RI, MS
38	β-Calacorene	1548	1547	1936	0,5	0,3	0,2	0,4	0,2	0,2	0,2	RI, MS
39	E-Nerolidol	1546	1551	2037	0,4	1,3	1,7	1,4	1,6	1,1	2,1	RI, MS
40	epi-Globulol	1558	1559	2010	0,6	tr	0,3	0,6	0,3	0,4	0,4	RI, MS
41	Caryophyllene oxyde	1576	1571	1980	3,2	1,4	2,1	3,1	2,1	2,5	3,5	RI, MS
42	Z-Nerolidol	1518	1521	1987	0,3	0,1	0,2	0,4	0,5	0,2	0,3	RI, MS
43	Germacrene D-4-ol	1573	1566	2020	0,7	4,4	2,5	1,8	1,1	3,4	1,2	RI, MS
44	Globulol	1580	1576	2067	0,4	0,5	1,9	0,7	1,3	1,7	0,4	RI, MS
45	Humulene epoxyde	1592	1601	2044	1,1	0,4	0,7	0,5	0,4	0,1	1	RI, MS
46	β-Oplopenone	1593	1590	2017	1,2	2,6	1,1	4,1	1,3	2,2	3,2	RI, MS
47	Viridflorol	1591	1591	2089	4	4,5	3,9	2,6	3,1	5,8	4,5	RI, MS
48	Zingeberenol	1598	1599	2019	0,5	0,8	0,6	0,4	0,3	0,1	1	RI, MS
49	1,10-diepi-Cubenol	1608	1608	2025	0,4	1,1	1,3	1,3	1,2	1,2	0,8	RI, MS
50	Aromadendrene epoxyde	1615	1617	2002	0,4	1,2	1,3	1,5	1,1	0,8	1,4	RI, MS, Ref
51	Eudesma-4(15)-en-6-one	1616	1614	2039	1,4	0,3	1,2	1,5	1,1	1,3	0,5	RI, MS
52	Cadin-4-en-7-ol	1627	1627	2096	1,1	0,5	0,6	1,6	1,2	1,6	1,1	RI, MS
53	Trans-Murolol	1630	1630	2134	0,6	0,5	0,4	0,2	0,5	0,6	1,2	RI, MS
54	tau-Cadinol	1632	1632	2169	6,7	9,5	8,4	6,6	9,1	5,6	6,7	RI, MS
55	β-Eudesmol	1638	1644	2234	0,5	0,3	tr	tr	tr	0,3	2,4	RI, MS
56	α-Carinol	1644	1645	2231	tr	tr	tr	tr	tr	tr	0,2	RI, MS
57	α-Cadinol	1645	1642	2231	12,2	12,3	16,1	15,2	18,8	15,3	12,2	RI, MS
58	Z,Z-Farnesol	1648	1653	2167	1,2	1	0,9	0,7	0,2	0,5	2	RI, MS
59	α-Eudesmol	1653	1649	2220	1,8	1,8	1,1	1,6	1	1,8	1,1	RI, MS
60	β-Bisabolol	1656	1653	2140	1,2	0,8	0,9	0,7	0,5	1,2	1,3	RI, MS, Ref
61	ar-Curcumen-15-al	1681	1675	2164	3,4	1,5	1,9	1,6	1	3	3,9	RI, MS
62	Eudesma-7,11-en-4-α-ol	1683	1683	2300	0,6	0,3	0,1	0,5	0,2	tr	2	RI, MS
63	**Shyobunol**	1687	1688	2218	19,7	23,9	21,1	20,5	19,1	19,5	10,5	RI, MS
64	Ledol	1696	1693	2050	2,1	0,3	2	0,7	1,8	1,1	**4**	RI, MS
65	E-Nerolidol acetate	1732	1738	2269	5,4	2,7	3,2	1,4	3,1	4,9	0,9	RI, MS, Ref
66	β-Acoradienol	1797	1792	2221	6,4	0,9	2,1	4,3	2,1	1,1	2,1	RI, MS
67	Z,E-Farnesyl acetate	1840	1832	2356	0,4	0,2	1,5	0,4	0,3	0,2	6,4	RI, MS
68	Heptadec-8,11,14-trien-2-one	1871	1871	2330	1,6	4,1	1,3	0,4	0,5	3,7	0,4	RI, MS
69	E,E-Farnesyl acetate				1,6	4,1	1,3	0,4	0,7	5,4	1,2	
	Total Identification %				99.2	98.6	99.6	98,7	99.3	99.3	97,2	
	Yields % (w/w)				0.09	0.02	0.06	0.18	0.1	0.09	0.01	
	Hydrocarbon compounds				18	15,8	17,3	18,2	21,4	12,9	16,7	
	Sesquiterpenehydrocarbons				18	15,8	17,3	18,2	21,4	12,9	16,7	

(continued)

Table 2. Continued.

No	Components	$IRI_a{}^b$	RIa c	RIpd	S1	S2	S3	S4	S5	S6	S7	Identification
	Oxygenated compounds				75,3	75,6	76,5	72,2	73,3	80,6	80,5	
	Oxygenated monoterpenes				0,5	tr	0,9	0,3	0,8	0,4	0 ,6	
	Oxygenated sesquiterpenes				74,3	75,4	74	71,4	72	79,9	79,9	
	Non-terpenic oxygenated compounds				0,5	0,2	1,6	0,5	0,5	0,3	0,6	

Table 3. % Inhibition of DPPH• of aerial part of *I. montana* essential oil and ascorbic acid at different concentrations.

Samples		Antioxidant activity					
Essential oil	Concentration (mL/L)	**0.04**	**0.05**	**0.06**	**0.075**	**0.09**	
	DPPH Radical scavenging activity [%]	33.06	42.01	49.75	63.6	78.57	
	IC_{50} (mL/L)						0.059
Ascorbic acid	Concentration (mL/L)	**0.04**	**0.05**	**0.06**	**0.07**	**0.08**	
	DPPH Radical scavenging activity [%]	36.03	47.95	61.27	75.32	90.7	
	IC_{50} (mL/L)						0.051

(Giamperi et al.., 2010) and Malta (26.2%) (Tsoukatou & Roussis, 1999). Then that of Greece (Tsoukatou & Roussis, 1999) by β-Phellandrene (30.7%) and that of Sicily (Italy) (Fontana et al., 2014) by thymol (11.8%). The essential oil of *I. germanica* and *I. bifrons* collected in Bulgaria (Trendafilova et al., 2020) was composed by cis-Carvyl acetate (20.7%) and Muurola-4,10 (14) dien-1-ol (8.6%) respectively, and that of *I. graveolens* from Turkey(Kiliç, 2014) was constituted by 1,8-cineole (22.4%). Note that the variation in the composition of essential oils could be due to several factors; the climatic conditions of the season of sample collection, the water supply, the nature and composition of the soil as well as insect attacks that can influence the chemical composition of essential oils (Baser & Buchbauer, 2010). From our results cited in Table 2, we were able to trace the variation in the contents of the different chemical classes of essential oils from other *I. Montana*.

The histogram (See Supplementary Materials Figure S1) showed that the essential oil is rich in oxygenated sesquiterpenes (74.3%), the percentage of hydrocarbon sesquiterpenes is relatively lower (18%) compared to oxygenated sesquiterpenes. However, oxygenated monoterpenes (0.5%) and oxygenated non-terpene components (0.5%) constitute the lowest percentage classes.

3.1.2. Evaluation of the antioxidant activities of essential oil

The Antioxidant power was performed by the DPPH free radical scavenging and the ferric reducing antioxidant power (FRAP) tests using ascorbic acid as a positive control. The comparison of the DPPH scanning activity of the essential oil of *I. montana* with that expressed by ascorbic acid showed good antioxidant activity. Indeed, the essential oil has the ability to reduce the DPPH radical to 78.57% with a concentration of around 0.09 mL/L (Table 3).

Figure 2 represent the absorbance values as a function of different concentrations of essential oil obtained by the FRAP method. The antioxidant power of the essential oil increases with increasing concentration. However, at 0.15 mL/L, the antioxidant activity of the essential oil was greater than of the synthetic antioxidant (ascorbic acid) (Fig.2).
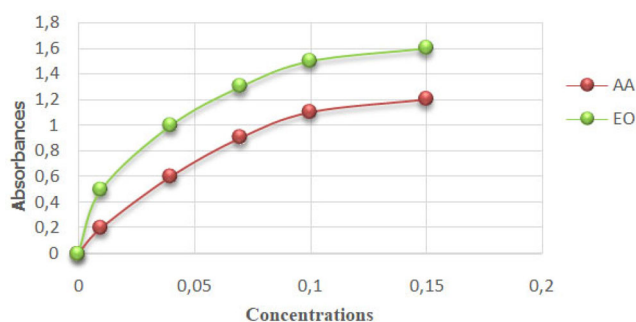
Figure 2. Reducing power activities of *I. montana* essential oil (EO), and Ascorbic acide.

3.2. Theoretical and computational methods

The ligands of essential oils from the Aerial parts of *I.montana* minimized toxicity and energy obtained by *MOE software* are shown in (Table 4). Properties for other compounds (See Supplementary Materials Table S1)

As stated in the table above. We find that the molecules Z,E-Farnesyl acetate, E-Nerolidol acetate, E, E-Farnesyl acetate, and E-β-Farnesene have a high value of Log P and Log S compared to other molecules and also the results obtained show that these ligand molecules (Z,E-Farnesyl acetate, E,E-Farnesyl acetate, E-Nerolidol acetate and E-β-Farnesene have a high value of torsion angle relative to other compounds. This shows that these compounds L67, L69, L65, L23 and L56 are more flexible. As well, it is noted that the growth of the torsion angle depends on the binding number of the molecule.

3.2.1. Binding affinity of compounds with superoxide dismutase target

3.3. Evaluation of molecular docking

3.3.1. Interaction with superoxide dismutase

We note that the result obtained (Table 5, 6),out of the best compounds studied E,E-Farnesyl acetate (Ligand 69) (Fig. 3) was predicted to be the strongest Superoxide Dismutase binder that forms a complex with the most stability with the lowest energy −4.401/mol. The ligands that interact with

Table 4. Some properties of best compounds For Antioxidants Drug.

Ligand compound		Toxic	LogP	Energies (Kcal/mol)	LogS	Hdon + Hacc	Flexibility
L32	E,E-α-Farnesene	No	5.20	2.18401e + 001	−6.01	don:0; acc:0	2 out 2
L27	α-Curcumene	No	4.84	3.01079e + 001	−5.22	don:0; acc:0	4 out 4
L30	Zingebrene	No	4.89	2.59488e + 001	−4.87	don:0; acc:0	4 out 4
L34	trans-Calamenene	No	4.69	4.34534e + 001	−5.80	don:0; acc:0	1 out 1
L42	Z-Nerolidol	No	4.40	2.11435e + 001	−3.93	don:1; acc:1	7 out 7
L56	α-Carinol	No	1.23	8.54556e + 001	−2.09	don:5; acc:7	9 out 9
L65	E-Nerolidol acetate	No	4.97	2.66094e + 001	−4.55	don:0; acc:1	9 out 9
L66	β-Acoradienol	No	3.70	4.03789e + 001	−4.64	don:1; acc:1	2 out 2
L67	Z,E-Farnesyl acetate	No	4.97	1.57696e + 001	−4.87	don:0; acc:1	9 out 9
L69	E,E-Farnesyl acetate	No	4.97	1.53201e + 001	−4.87	don:0; acc:1	9 out 9

Results of Energy balance of best complexes formed with *SODs* target are given in (Table 5). Energy for other compounds (See Supplementary Materials Table S2).

Table 5. Results of Energy balance of best complexes formed with Antioxidants Drug molecules.
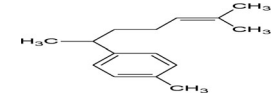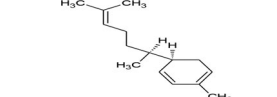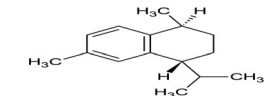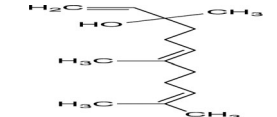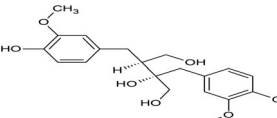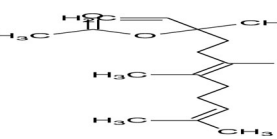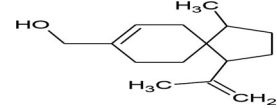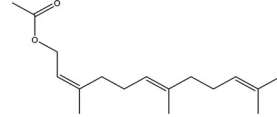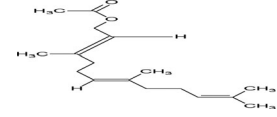
	Chemical structure	Binding energy (Kcal/mole)	Rmsd -refine	Energy-conf	Energy- place	Energy-refine	RMSD
E,E-α-Farnesene		−3.915	1.511	−1.997	−5.738	−3.758	1.154
α-Curcumene		−4.093	1.503	35.082	−0.102	−12.536	0.214
Zingibrene		−4.032	2.021	36.990	25.109	−13.224	0.198
Trans- -Calomenene		−4.100	2.831	44.135	−33.581	−9.968	0.434
Z-Nerolidol		−4.000	3.403	−10.987	−1.967	−10.604	0.116
α-Carinol		−4.150	3.192	3.192	75.237	−17.291	0.984
E-Nerolidolacetate		−4.226	5.681	33.046	−2.144	−10.626	1.101
β-Acoradienol		−4.011	1.236	38.401	−12.797	−12.301	0.476
Z,E-Farnesyl acetate		−4.175	2.665	23.760	−14.341	−10.152	1.007
E,E-Farnesyl acetate		−4.401	3.665	−22.011	1.348	−11.109	0.539

Table 6. Results of bonds between atoms of compounds and active site residue of the Superoxide Dismutase (SODs).

N°	Compounds	S-score	Atom of compound	Involved receptor atoms	Involved receptor residues	Type of interaction bond	Distances (Å)	Energies (kcal/mol)
	Superoxide Dismutase(SOD)							
L27	α-Curcumene	−4.093	6-ring	O	HOH 2043	pi-H	4.24	−0.7
L54	tau-Cadinol	−4.087	O1 1	OG	SER 98	H-acceptor	2.91	−1.6
L56	α-Carinol	−4.150	6-ring	CD	LYS 30	pi-H	4.57	−0.6
L66	β-Acoradienol	−4.011	O1 1	O	HOH 2051	H-donor	2.52	0.7
			O1 1	O	HOH 2042	H-acceptor	2.43	5.1
L2	Z-Hex-3-en-1-ol	−3.212	O1 1	5-ring	TRP 32	H-pi	3.81	−0.7
L6	Octanal	−3.300	O1 1	ND2	ASN 19	H-acceptor	3.15	−1.3
L20	E-β-Caryophyllene	−3.154	O1 1	NE1	TRP 32	H-acceptor	3.50	−0.5
L39	E-Nerolidol	−3.752	O1 1	O	HOH 2130	H-donor	2.61	−0.6
L40	epi-Globulol	−3.438	O1 1	O	HOH 2128	H-acceptor	2.73	−1.1
L46	β-Oplopenone	−3.354	O1 1	OG	SER 98	H-acceptor	2.48	2.9
L47	Viridiflorol	−3.677	O1 1	O	HOH 2126	H-acceptor	2.53	−0.1
L53	Trans-Murolol	−3.655	O1 1	OG	SER 98	H-acceptor	2.90	−1.6
L55	β-Eudesmol	−3.578	O1 1	O	HOH 2043	H-acceptor	2.97	−0.6
L59	α-Eudesmol	−3.571	O1 1	O	HOH 2043	H-acceptor	2.97	−0.6
L63	Shyobunol	−3.433	O1 1	NZ	LYS 75	H-acceptor	3.34	−1.5
L65	E-Nerolidol acetate	−4.226	H2	O2	HOH2043	WaterH-bond	2.10	−0.9
			C14	O	LYS30	Alkyl Interaction	4.83	−1.2
			C18	O	LYS75	Alkyl Interaction	2.87	−0.5
			C19	O	LYS75	Alkyl Interaction	4.87	−1.1
L67	Z,E-Farnesyl acetate	−4.175	C15	O	LYS30	Alkyl Interaction	4.83	−1.2
L69	E,E-Farnesyl acetate	−4.401	H1	O2	HOH2043	Water H-bond	2.21	−0.6

H = Conventional hydrogen bond, C = Carbon hydrogen bond, Aa = Alkyl-alkyl, Ap = Alkyl-Pi, Aps = Amide-Pi stacked, Ppt = Pi-pi T-shaped, X = Halogen.
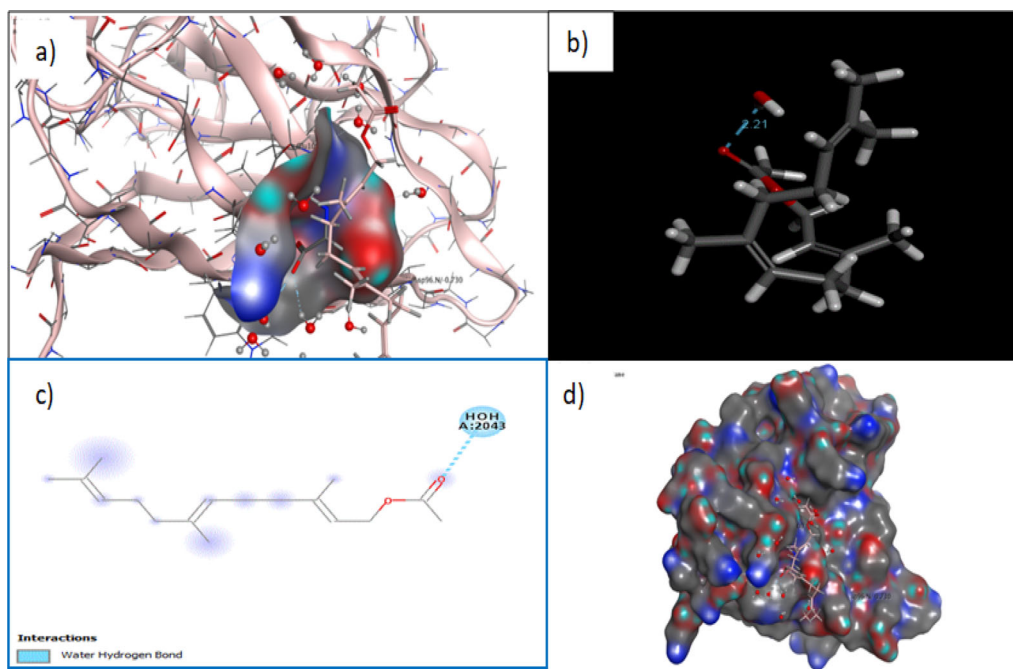

Figure 3. Displaying the Superoxide Dismutase binding site cavity 3 D interaction diagram of E,E-Farnesyl acetate with pocket(a) and without pocket (b) ; Binding mode of E,E-Farnesyl acetate as 2 D diagram (c);The binding patterns E,E-Farnesyl acetate in the active site of Superoxide Dismutase, in which E,E-Farnesyl acetate is disappeared in stick model with pink while the surface of SOD is shown in blue red green (d).

Superoxide Dismutase are: α-Curcumene Ligand L27 interacts with HOH 2043 at a distance of 4.24 Å strong with energy of-0.7 and tau-Cadinol ligand L54 interacts with one amino acid SER 98 H- acceptor at a distance of 2.91 Å strong and energy binding of −1.6, similarly, the β-Acoradienol ligand L66 interacts with HOH 2051 HOH 2042, (H-acceptor, H-donnor) at a distance of (2.52,2.43)Å respectively strong, low. Z-Hex-3-en-1-ol Ligand L2 interacts with TRP 32H-pi at a distance of 3.81 Å weak and energy binding of −0.7and methyl-hept-5-

en-2-one Ligand L46 interacts with one amino acid TRP 32 H-acceptor at a distance of 3.30 Å strong and energy binding of −0.7. It is noted that the interactions between the residues of the active site of 2wz5 and E, E-Farnesyl acetate ligand form a stable complex.

The second-best binder was E-Nerolidol acetate (Ligand65) with the energy of −4.226 Kcal/mol) that interacts with HOH 2043 H-acceptor at a distance of 3.05 Å strong interaction and energy binding of −0.9 Kcal/mol (Fig. 4). The ligands that interact
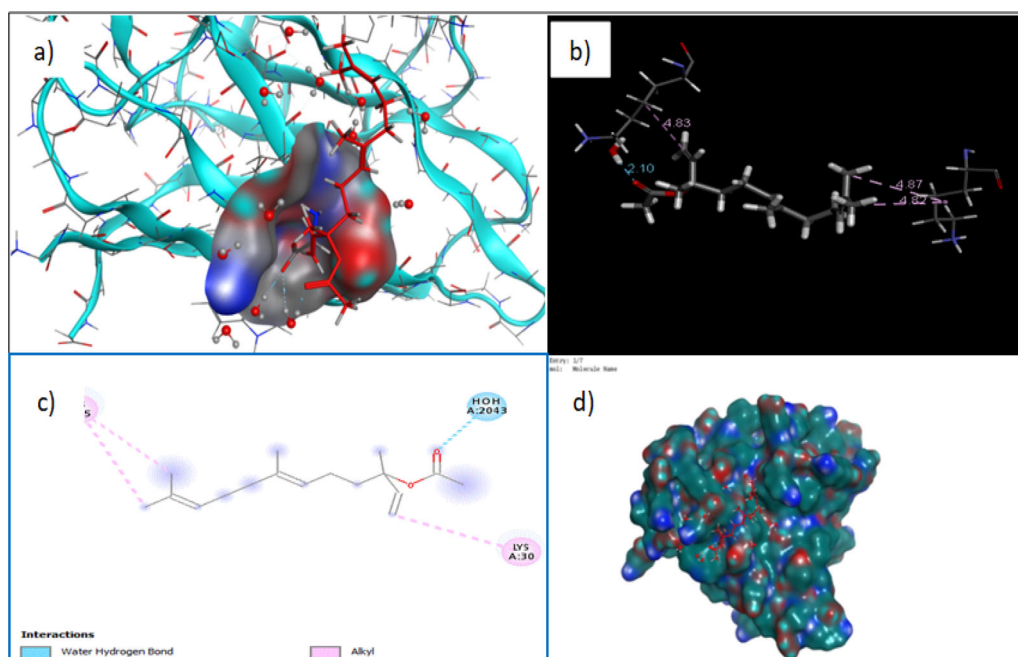
Figure 4. Displaying the Superoxide Dismutase binding site cavity 3 D interaction diagram of E-Nerolidolacetate with pocket(a) and without pocket (b) ; Binding mode of E-Nerolidolacetate as 2 D diagram (c);The binding patterns E-Nerolidolacetate in the active site of Superoxide Dismutase, in which E-Nerolidolacetate is disappeared in stick model with pink while the surface of SOD is shown in blue red green (d).

Table 7. The docking energies of *DNA* inhibitors.

	Compound	DE*(kcal/mol) ctDNA	DE*(kcal/mol) Enzyme	ETOR (kT)	VDW (kT)	EIE (kT)
Control ligand	Ascorbic acid	−4.383	−3.329	345.417	553.157	−1639.53
Lref	L-methionine	−4.277	−3.388	331.046	412.988	−1941.78
L69	E ,E Farnesyl acetate	−6.855	−4.401	331.636	412.865	−1941.94
L67	E ,Z Farnesyl acetate	−6.336	−4.175	331.503	412.724	−1941.62
L56	α-Carinol	−6.276	−4.150	330.732	413.030	−1942.17
L65	E-Nerolidol acetate	−6.087	−4.226	345.417	553.157	−1639.53
L32	E,E-α-Farnesene	−6.084	−3.915	331.636	412.864	−1941.94
L27	α-Curcumene	−5.727	−4.093	330.612	413.093	−1942.17
L42	Z-Nerolidol	−5.569	−3.980	330.570	412.976	−1942.21
L34	trans-Calamenene	−5.498	−4.100	330.567	412.975	−1942.22
L30	Zingebrene	−5.176	−4.032	330.174	413.373	−1942.50
L66	β-Acoradienol	−4.742	−4.011	330.719	412.932	−1942.20

*DE: Docking Energy; ETOR: torsionEnergy; VDW: Van der Waals; EIE: Electrostatic Interaction Energy.

with Superoxide Dismutase *are:* E-β-Caryophyllene, Trans-Murolol and Shyobunol interacts with one amino acid ASN19, TRP3, 2 SER98 and LYS75 H-acceptor at a distance of 3.15,3.50,2.48 and 3.34 Å averages, strong interaction and energy binding of −1.3, −0.5,2.9 and −1.5 Kcal/mol And interaction with E-Nerolidol, epi-Globulol, Viridiflorol, β-Eudesmol and α-Eudesmol with HOH 2130, HOH 2128, HOH 2126 and HOH 2043 respectively. H-donnor and H-acceptor at a distance of 2.61,2.73,2.53 and 2.97 Å strong, low, average interaction and energy binding of −0.6,-1.1,-0.1 and −0.6 Kcal/mol respectively. This suggests that E-Nerolidol acetate can inhibit Superoxide Dismutase. Results of docking calculations and bonds between atoms of compounds and residues of the active site are given in Table 6.

Binding affinities and non-bonding interactions are listed in Table 3. The additions of halogen not only increase the physicochemical properties but also binding affinity and speciality (Nair et al., 1994). The incorporation of –CF3 group increased inhibiting and medicinal properties (Abu Saleh et al., 2016; Plano et al., 2016). Group carbon trifluoride has great

significant applications in the field of agronomical dyes, pigments, pharmaceuticals, polymers and material science when it is incorporated to different organic molecules due to the strong electronegative and hydrophobic characteristics, which can be used in drug design to improve the selective functionality (Lishchynskyi et al., 2013; McClinton & McClinton, 1992).

In our study, all the compounds show several significant hydrogen bonds. Some recent studies reported that, halogen bonding similar to hydrogen bonding plays crucial role for biological and chemical system (Sarwar et al., 2010; 2013). The binding affinity of L69, L65, L67, L56, L27 and L54 have considerably increased to −4.401, −4.226, −4.175, −4.150, −4.093, and −4.087 kcal/mol respectively of E,E-Farnesyl acetate, E-Nerolidol acetate, Z,E-Farnesyl acetate, α-arinol α-Curcumene, and tau-Cadinol. Improved hydrogen bond is observed in L69 and L65 not only contricbute in increasing binding affinity but also enhance the binding specificity (Bissantz et al., 2010; Sarwar et al., 2013). This observation helped to confirm that (Oxygenated sesquiterpenes) and
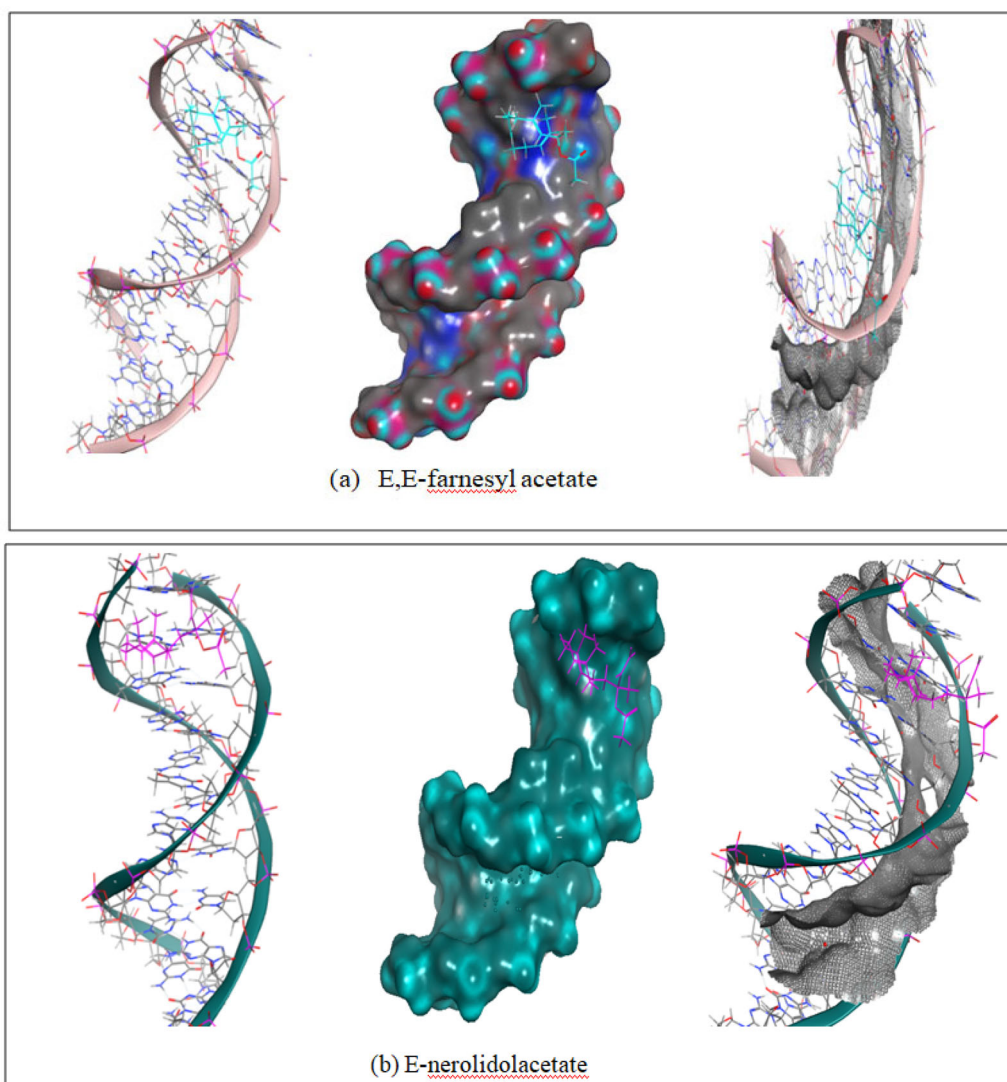
Figure 5. Molecular docked model of the most favorable binding site of compounds (a) L69 and (b) L65 with DNA dodecamer duplex of sequence d (CGCGAATTCGCG)2 (PDB ID: 1BNA).

compounds (D67, D56 and D27) are binding at the desired binding site of receptor protein after molecular docking.

3.3.2. Interaction with DNA sequence

Free radicals, especially OH °, can attack DNA. They react with nucleotides. They can lead, for example, to changes in nitrogen bases, DNA fragmentation, strand breaks or base bridging. Therefore, they would be needed in the development of diseases such as cancer, neurodegenerative diseases and the pathogenesis of viral infections. The accumulation with age of radicals and therefore the damage they generate would be one of the factors explaining cellular aging . The drug was successively docked with DNA duplex of sequence d(CGCGAATTCGCG)2 dodecamer (PDBID:1BNA) and is shown in (Table 7)

Our results demonstrated that the four compounds: E-β-Farnesene (Ligand 23), α-Carinol (Ligand 56), E-Nerolidol acetate (Ligand 65) and E;E Farnesyl acetate (Ligand 69) were the best interacting compounds (see Table 7). The calculated docking energies for these compounds were respectively −6.009, −6.276, −6.087 and −6.114 kcal.mol^{-1}. With the

exception of tau-Cadinol and β-Acoradienol, other compounds are located in the small cDNA groove.

The results of molecular docking showed that tau-Cadinol and β-Acoradienol existed in the main groove region. The calculated docking energy of this compound was −4.708 and −4.742 respectively kcal.mol^{-1} (see Table 5).

Binding energy is the primary parameter which is generated as a result of molecular docking. It gives us the idea of strength and affinity of the interaction between the ligand and the receptor. The greater the binding energy is, the weaker the interaction is and vice versa. Thus, during any docking study, we intend to look for the ligand which displays the least binding energy, thus the best affinity among the test molecules (Nisha et al., 2016). Among the test candidates in this study, E,E Farnesyl acetate and E-Nerolidol acetate displayed the lowest binding energy of −6.865 and −6.087 kcal/mol for DNA sequence and −4.733 and −4.226 kcal/mol for enzyme . The binding energy of the Lref (−3.388 kcal/mol for the enzyme and the control ligand; ascorbic acid (−4.383 kcal/mol for DNA sequence and −3.329 kcal/mol for the enzyme were much higher than E, E Farnesyl acetate, as found in our study; thus Farnesyl acetate and E-Nerolidol acetate

Table 8. Thermodynamic properties calculated in reels units.

Stage	Method	H	U	EKT	P	V
SP$_1$	PEROX1NVT	−165.222	−1121.029	2397.107	−259.305	21731.382
	PEROX2NPT	36.306	−2679.731	1027.389	−57.269	417.362
	PEROX1NVT	1.584	−2233.072	1930.936	−184.288	21731.382
	PEROX2NPT	1.320	−2874.760	1199.694	−58.531	218.488
	PEROX1NVT	−1.367	−2258.180	1976.864	296.146	21731.382
	PEROX2NPT	−0.943	−2929.258	1269.987	−52.646	501.078
SP$_2$	PEROX1NVT	−2273.905	1975.170	1297.141	286.447	21057.382
	PEROX2NPT	0.835	−2909.660	1252.199	−57.083	601..500
	PEROX1NVT	2.523	2356.218	2016.582	114.555	21757..382
	PEROX2NPT	92.991	−2923.494	1358.883	−49.508	129..876
	PEROX1NVT	3.171	−2332.877	2332.877	148.306	21761.382
	PEROX2NPT	−1903.034	−5548.395	1990.654	−58.157	700.555
SP$_3$	PEROX1NVT	1986.618	−2372.214	1986.618	−125.724	21731.382
	PEROX2NPT	−1993.422	−5682.353	2034.241	−59.258	680.882
	PEROX1NVT	2.226	−2339.252	1965.961	−136.010	21731.382
	PEROX2NPT	−3045.507	−2253.922	2253.925	−57.256	351.001
	PEROX1NVT	1.678	−2429.067	1953.394	−132.638	21731.382
	PEROX2NPT	−5154.32	−5839.098	3174.523	−53.748	143.483

Pressure $P = P^* \, \varepsilon / \, \sigma^{-3}$. Energy of configuration $U = U^* \, N\varepsilon$. Translation Kinetic Energy $EKT = EKT^* \, N\varepsilon$ and Enthalpy $H = H^* \, N\varepsilon$.

displayed much better binding than the Lref and control molecule; ascorbic acid (See Supplementary Materials Figure S2).

The more negative relative binding energy for E,E Farnesyl acetate indicated greater binding tendency of this compound with DNA. Thus the results obtained from docking molecular studies were found to be consistent with molecular dynamics simulation studies, which can validate our simulation findings. Both docking and dynamics studies suggest that compound E,E Farnesyl acetate has a strong DNA-binding affinity than compound E-Nerolidol acetate. The additional acetate group of compound E,E Farnesyl acetate makes specific hydrophobic interactions with nucleotide bases of DNA. Moreover, docking studies also suggested that a large part of binding energy is derived from hydrophobic interactions. From these results, it should be noted that several factors, notably the variability of the ligand structures and the capacity to build covalent and/or non-covalent bonds, could affect their binding affinity to the small cDNA groove.

There are even other factors such as the distribution of electrostatic charges with DNA and also the base pairs A: T (Neidle, 2001). Studies have suggested that minor groove binding ligands carry a cationic charge, complementing the potential in A: T regions. Our results are fully consistent with previous reports and the compounds studied interacted with A: T base pairs. E, E Farnesyl acetate, and E-Nerolidol acetate displayed much better binding. (see Fig.5).

3.3.3. Interaction with endogenous enzymatic antioxidant systems

3.3.3.1. The case of superoxide dismutase (SODs).
Antioxidants can be classified into fat soluble or water soluble molecules. According to their physicochemical characteristics, they will have a preferential cellular localization: the cell membranes for the liposoluble substances and the cytosol and/or the extracellular medium for the water-soluble substances. They will be particularly effective on the free radicals present in each type of medium, respectively (See Supplementary Materials Figure S3). The results of docking energies of Superoxide Dismutase (SODs) best inhibitors are shown in (See Supplementary Materials Table S3). And results of other compounds are shown in (see supplementary Table S3.a).
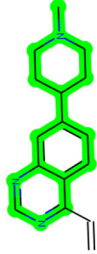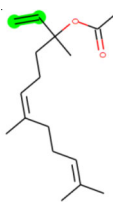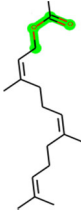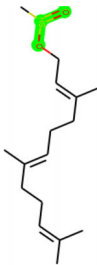
The exogenous defenses (Superoxide dismutases, Catalase, Glutathione peroxidase) seem the easiest to support since they could be strengthened by the intake of food supplements. Superoxide dismutases: Converts free radicals to less damaging substances, such as Hydrogen peroxide. Catalase: Removes hydrogen pyroxide from the body. Glutathione peroxidase: Removes hydrogen peroxide. Molecular docking results revealed that trans-Calamenene (Ligand 34), α-Carinol (Ligand 56), Zingebrene (Ligand 30) E-Nerolidol acetate (Ligand 65), Z,E-Farnesyl acetate (Ligand 67) and E,E-Farnesyl acetate (Ligand 69) were the best compounds interacting with the suspected binding residues at the active site Superoxide Dismutase (See Supplementary Materials Figure S4). The calculated docking energies of these molecules were respectively −4.100, −4.150, −-4.322, −4.226, −4.175 and −4.401 kcal.mol^{-1}. Z-Nerolidol and E,E-α-Farnesene was the weakest interacting compound with this receptor. The calculated docking energy of these compounds is: −3.980 and −3.915 kcal.mol^{-1}, respectively. The docking parameters include free binding energy, intermolecular energy and torsional free energy values were calculated. We observed that E,E-α-Farnesene (Ligand 32), α-Curcumene (Ligand 27), α-Carinol (Ligand 56), and E-Nerolidol acetate (Ligand 65) E,E-Farnesyl acetate (Ligand 69) and Z, E-Farnesyl acetate (L67) showed a binding affinity for interacting with receptors for cDNA, and trans-Calamenene (L34), α-Carinol (Ligand 56), Zingebrene (Ligand 30), E-Nerolidol acetate (Ligand 65) E,E-Farnesyl acetate (Ligand 69) and Z, E-Farnesyl acetate (Ligand 67) showed a binding affinity for interacting with receptors for Superoxide Dismutase. 3 D representations of the best pose interactions are shown in (See Supplementary Materials Figure S4). The results given, we can conclude that the best inhibition this product by two molecules E-Nerolidol acetate (Ligand 65) and E,E-Farnesyl acetate .

3.4. Evaluation of molecular dynamics

3.4.1. Thermodynamic properties
Thermodynamic properties using the MD simulation approach, we have studied the evolution thermodynamic

Table 9. In silico Bioisosteric Replacement based on similarity comparison method.

Molecule	Replacable group	Transformation in previous studies	Analogue structure	Smiles
L65	[structure]	//	1-Analog L65 [structure]	CN1CCC(C2=CC=C3C(C=NN=C3C)=C2)CC1
	[structure]	J. Med. Chem., 2015, 58, 9625-9638 J. Med. Chem., 2014, 57, 1208-1224 Eur. J. Med. Chem., 2014, 80, 295-307	2-Analog L65 [structure]	O=C(C)OC([NH3+])(C)CC/C=C(C)/CC/C=C(C)/C
L69	[structure]	//	1-Analog L69 [structure]	O=[SH](C)OC/C=C(C)/CC/C=C(C)/CC/C=C(C)/C

Note: the molecule, replaceable group, and analogue structure cells contain chemical structure diagrams.

properties of best ligand, E,E-Farnesyl acetate in NVT and NPT ensemble (Table 9). We performed energy minimizations of the best complex after docking of 600ps. Then carried out simulations up to (MD production cycles) 100 ns in three stages under constraints (see table 8).

Initiation stage sp1 20 ns Heating (thermalization) from 0 to 300 K for example

Equilibration stage sp2 20 ns -40ns Normal simulation, but the system is not in equilibrium. 40 ns-60ns relaxation (adaptation) of water on the surface of the protein

Production stage sp3 60 ns-100ns we saved the trajectories

Analyzes Finally, the analysis of the results and validation by contributing to the score (energy) obtained by docking.

The results represented in table 7 revealed that the kinetic energies of translation and the internal energy for the E,E-Farnesyl acetate (Ligand 69) in NVT and NPT ensemble. In the *Superoxide dismutases* (*SODs*) enzyme in NVT units, are low compared to the *Superoxide dismutases* (SODs) receptors in NPT units. And the fluctuation in pressure for the complex receiver is significant. Therefore, E,E-Farnesyl acetate (Ligand 69) are predicted to be the most interactive system. These results are in total agreement with the Docking prediction results(see Tables 4-5).We can show the detailed analysis of MD simulation results of only compound E,E-farnesyl acetate (Ligand 69) with target *Superoxide dismutases* (*SODs*) enzyme (Fig. 6 and 7).

3.4.2. Structural dynamics properties

Structural Dynamic properties using the MD simulation approach, we have studied the evolution structural dynamics of the best ligand molecule L69 (See Table 5) by IMODS.

The normal mode analysis (NMA) of the prepared E,E-Farnesyl acetate- Superoxide Dismutase(*SODs*) complex was illustrated in (Fig. 8a) From the molecular dynamics study of the prepared E,E-Farnesyl acetate - Superoxide Dismutase(*SOD*) complex, it was clear that the prepared enzyme-ligand complex had a quite high eigenvalue of 2.446366e-04 the eigenvalue is illustrated in (Fig. 8b). However, the variance map showed a high degree of cumulative variances than individual variances (Fig. 8c). The co-variance and elastic network map also produced quite satisfactory results (Fig. 8d, and Fig. 8e) respectively. The deformability graphs of the complex (E,E-Farnesyl acetate-Superoxide Dismutase(*SODs*) illustrate the peaks in the graphs correspond to the regions in the protein with deformability (Fig. 8f). The two selected ligand molecules can be used as potential agents to deplete DPPH and free radicals. Overall, in our study, E,E-Farnesylacetate emerged as the most potent anti- Superoxide Dismutase(*SOD*) agent. However, more *in vitro* and *in vivo* researches should be performed on the E,E-Farnesyl acetate best ligands to finally confirm the findings of this study.

3.5. The OSIRIS property explorer

A computational study of best compounds was performed for the assessment of OSIRIS properties (See Supplementary Materials Table S4) Prediction results are valued and color coded.(Nalini et al., 2011). Properties with high risks of undesired effects like mutagenicity or a poor intestinal absorption are
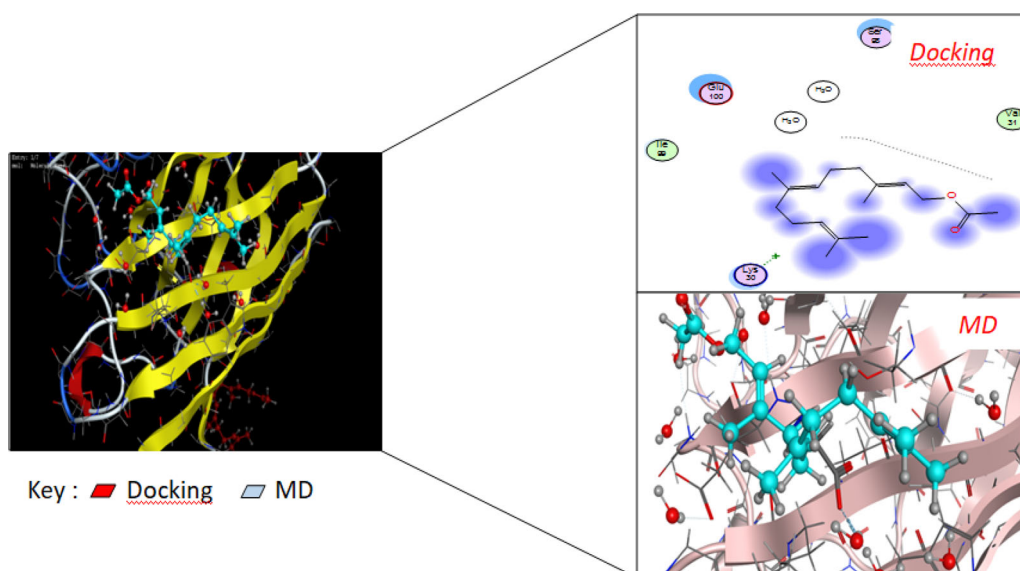
Figure 6. The compound – 69; E,E-Farnesyl acetate docked without water well into the binding site of *SOD* and has the highest dock score; there is also a clear difference between the final ligand pose and the docking pose after a molecular dynamics (MD) simulation in NVT.

Figure 7. The compound – 69; E,E-Farnesyl acetate docked without water well into the binding site of *SOD* and has the highest dock score; there is also a clear difference between the final ligand pose and the docking pose after a molecular dynamics (MD) simulation in NPT.
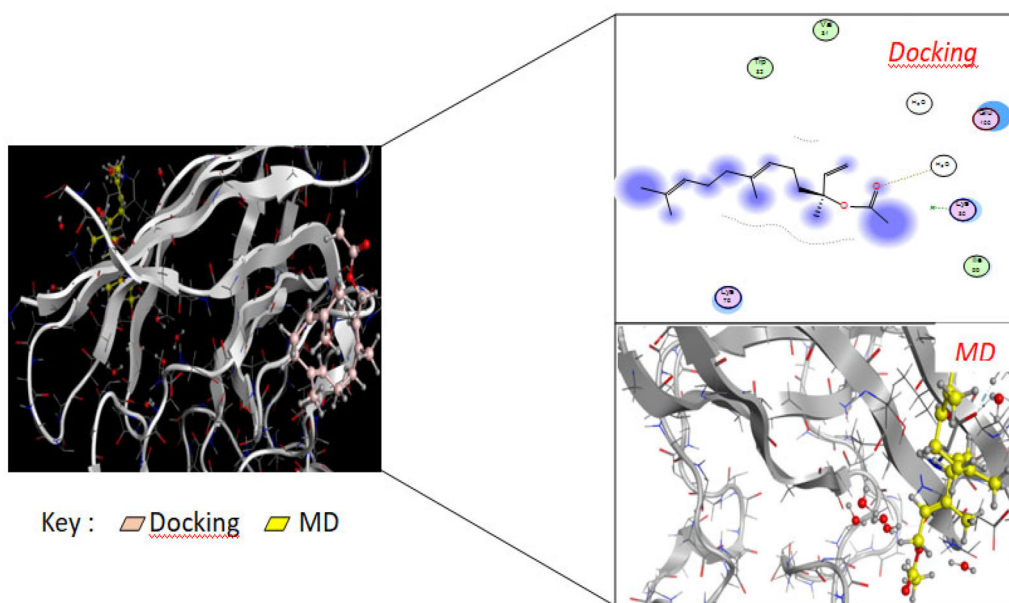
shown in red. Whereas a green color indicates drug-conform behavior. The results exposed in table 8 revealed that compounds (L32, L34 and L56) are the best ligands and L42 and L66 are only irritating. What interests us most are ligands L65 and L69 because the latter have well complementary with the enzyme. We see that L69 is irritant and moderately tumorigenic reproductive effective and L65 is tumorigenic. It is moderately irritant. So the solution is to replace a fragment.

3.6. Bioisosteric replacement

In order to solve the problems associated with the pharmacokinetics of drugs and eliminate unwanted side effects such

as toxicity and metabolic responsibilities. We used, for our best ligands L65 and L69, (see table 9) Molopt (A web server for drug design using bioisosteric transformation) which automatically generates analog lists by replacing molecular substructures with chemical groups with similar biological properties. The resulting set of transforming analogs can be evaluated for future synthesis in the future.

We could not carry on further with the in vitro and *in vivo* testing due to lack of the required facilities, and thus this study needs further *in vitro* and *in vivo* animal studies for the development and authentication of these probable potent inhibitors of E,E-Farnesyl acetate for reduction of oxidative stress.
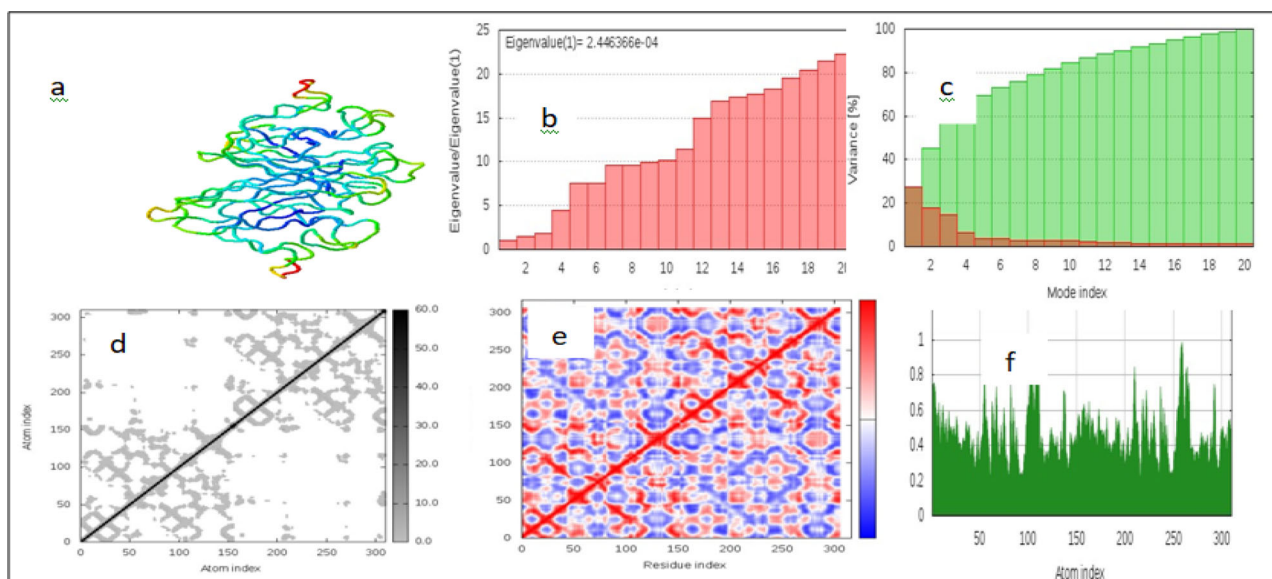
Figure 8. Results of molecular dynamics simulation of E,E-farnesyl acetate - Superoxide Dismutase(SOD) docked complex. (a) NMA mobility, (b) eigenvalue, (c) variance (red color indicates individual variances and green color indicates cumulative variances), (d) elastic network (darker grey regions indicate stiffer regions) of the complex, e) co-variance map (correlated (red), uncorrelated (white) or anti-correlated (blue) motions) and (f) deformability.

Table 10. Drug-likeness prediction through OSIRIS Property Explorer of best inhibitors (ligands).

S. number	Ligand	$c \log P$	Solubility log S	Molecular weight	TPSA Å^2	Druglikness	Drug score
Ascorbic acid		**−2.46**	**−0.35**	**176.12**	**107.22**	**0.02**	**0.75**
Lref		**−2.39**	**−1.05**	**149.21**	**88.62**	**−13.32**	**0.50**
01	L27	5.36	−3.81	202.34	00.00	−4.90	0.17
02	L30	5.06	−3.38	204.36	00.00	−3.02	0.08
03	L32	6.40	−3.31	204.36	00.00	−7.39	0.29
04	L34	5.19	−4.22	202.34	00.00	−8.18	0.36
05	L42	5.40	−3.13	222.37	20.23	−6.38	0.21
06	L56	1.66	−2.09	378.42	119.61	−1.63	0.52
07	L65	5.89	−3.54	264.41	26.30	−9.30	0.15
08	L66	3.70	−3.16	220.35	20.23	−24.21	0.26
09	L69	6.14	−3.28	264.41	26.30	−2.70	0.07
	1-Analog L65	2.5	−2.72	241.34	29.02	6.15	0.94
	2-Analog L65	1.12	−2.90	268.42	53.94	−4.86	0.39
	1-Analog L69	5.78	−3.62	285.47	26.30	−2.94	0.20

MW: molecular weight, MLogP: logarithm of partition coefficient of the compound between water and n-octanol: n-OHNH donors: number of hydrogen bonds donors. n-ON acceptors: number of hydrogen bond acceptors. n-ROTB: number of rotatable bonds.

Table 11. Pharmacokinetic and toxicity evaluated parameters of best compounds.

		65	Analog structure L65	Analog structure L65	69	Analog structure L69
Absorption	Human intestinal	93.999	95.602	95.251	93.643	92.869
	Skin permeability	−1.93	−2.496	−2.444	−1.896	−2.1
	Caco-2 permeability	1.64	1.646	1.501	1.632	1.609
	Surface Area	117.785	107.829	117.449	117.785	120.841
Distribution	VDss (human)	0.273	0.917	0.377	0.275	0.154
	Fraction unbound (human)	0.176	0.314		0.157	0.173
	BBB permeability	0.57	0.173	−0.201	0.621	0.637
	CNS permeability	−2.133	−2.065	−2.482	−1.973	−1.823
Excretion	Total clearance	1.752	0.869	0.958	1.749	1.957
	Renal Organic Cation transporter	No	No	No	No	No
Toxicity	Oral rat acute toxicity (LD50)	1.631	2.648	2.331	1.633	2.541
	AMES toxicity	No	No	No	No	No
	Tetrahymena Pyriformis Toxicity	2.251	1.211	1.053	2.344	2.527

green = good, yellow = tolerable , red = bad.
Active components: 65- E-nerolidolacetate, 69- E-E- Farnesylacetate. BBB: Blood-brain barrier. ADMET: Absorption. Distribution. Metabolism.and Excretion and Toxicity.
VD$_{SS}$: < -0.15 low, >0.45 high, BBB: >0.3 cross BBB, <-1 poorly distributed to the BBB, CNS: > -2 penetrate CNS, < -3 unable to penetrate CNS, Low skin permeability: > -2.5, Caco-2 permeability: > 0.9, Human intestinal absorption: > 90.

Table 12. The PASS prediction results showing the biological activities of the best two molecules.

		E,E-Farnesyl acetate L69		E-Nerolidol acetate L65	
SI no	Biological activities	Pa	Pi	Pa	Pi
01	Mucomembranous protector	0.973	0.002	0.976	0.002
02	CYP2E1 inhibitor	0.824	0.004	0.600	0.006
03	Macrophage colony stimulating factor agonist	0.729	0.010	0.582	0.037
04	Chemoprotective	0.562	0.006	0.496	0.015
05	Antioxidant	0.547	0.005	0.404	0.012
06	Antiulcerative	0.807	0.004	0.694	0.010
07	TNF expression inhibitor	0.779	0.004	0.610	
08	Antiviral (Rhinovirus)	0.754	0.002	0.734	0.002
09	ANTIFUNGAL	0.598	0.019	0.554	0.023
10	Membrane permeability agonist	0.540	0.008	0.588	0.094

3.7. In silico assessment of the ADME properties and drug-likeness

A computational study of best compounds was performed for the assessment of OSIRIS properties (Table 10).

The results exposed in table 10 revealed that compounds (L69 and L65) have high absorption with a low molecular weight of order 264.41. Also, we can note that these compounds comply with Lipinski's rule of 5.Veber's rule and Egan's rule. MW range 264.41 ($<$500), A log S value indicates solubility; the lesser the log S value, the higher the solubility, which would enhance the absorption log S for E-E- Farnesyl acetate and E-Nerolidol acetate are −3.28 and −3.54 respectively. A lower molecular weight would again enhance the absorption rate and thus most of the drugs are tried to be kept at the lowest possible molecular weight, suggesting that these compounds would not be expected to cause problems with oral bioavailability and thus showing the possible utility of both compounds for developing the compound with good drug like properties. Therefore, admetSAR will facilitate medicinal chemists to design and optimize lead compounds with better ADMET properties. We will continue to improve and extend the computational models for the prediction of chemical ADMET properties to make admetSAR a practical platform for drug discovery and other chemical research. Results of ADMET profiles of test ligand are given in (See Supplementary Materials Table S5). To date, it has been widely applied to drug discovery and environmental risk assessment, and has been cited by 207 times (Patel et al., 2018; Yang et al., 2018). It has also been embedded in Drug Bank since version 4.0 in 2014 (Law et al., 2014).

From the table 14 ADMET properties, as derived from admetSAR server (Cheng et al.., 2012) reveal that L69,L65 and L42 had better Human Intestinal Absorption (HIA) score than the Lref and ascorbic acid (0.9703, 0.9703 and 0.9645 versus 0.4786 and 0.8150). If a compound with the HIA% is less than 30%, it is labeled as HIA-, otherwise it is labeled as HIA+. Greater HIA denotes that the compound could be better absorbed from the intestinal tract upon oral administration. The penetration through the Blood-Brain Barrier (BBB) came out to be best for L69, L65 and L42 and was significantly higher than the control molecule and Lref (0.9932 and 0.9859 versus 0.9785 and 0.9384, resp.). L69 and L42 were a non substrate/non inhibitor while ascorbic acid was a non substrate/non inhibitor. But L65 was substrate/non inhibitor. A non inhibitor of CYP450 means that the molecule will not

hamper the biotransformation of drugs metabolized by CYP450 enzymes. The AMES toxicity test is employed to know whether a compound is mutagenic or not. Similar to the control molecule and Lref, all the test ligands displayed negative AMES toxicity test which means that the ligands are non mutagenic. Carcinogenic profile also revealed that the ligands were non carcinogenic similar to the control molecule and Lref, except for L32 wich present **Carcinogenicity**. Acute oral toxicity was found to be highest for ascorbic acid and Lref. All other test ligands had low and almost similar oral toxicity (between 1.3 and 3.2). Important information obtained from admetSAR server was the computed LD50 dose in a rat model. Comparing the LD50 doses, a compound with lower dose is more lethal than the compound having higher LD50. From our observation, we found that L69, L65 and L42 had the highest LD50, compared to the ascorbic acid (1.981, 2.276 and 2.768, resp.). Lref and ascorbic acid had the lowest LD50 of 1.235 and 1.318.

Apropos the absorption parameters compounds L65; and L69 present a promising oral availability, due to the optimal Caco-2 cell permeability and HIA ($>$ 0.9 and Human intestinal $>$ 90%. Respectively, Table11).

All compounds passed the AMES tests. The volume of distribution (VDss) for our two best ligands L65 and L69 are, respectively, 0.273 and 0.275 suggest that the drug will be distributed in plasma since the values of the VDss$< −0.15$. So, VDss describes the extent of drug distribution and the fraction unbound describes the portion of free drug in plasma that may extravasate. The compounds L65 and L69 may be interesting more potent antioxidative agents. The synthetic antioxidant ascorbic acid and the methionine co-crystallized inhibitor are entirely unable to penetrate the central nervous system (CNS).

The ligands antioxidant ascorbic acid and the methionine showed gastrointestinal absorption within acceptable limits. The absorption and distribution parameters, respectively, have been graphically represented by the extended and renewed version of the Edan-Egg model named Brain Or Intestinal Estimated (BOILED) permeation predictive model (BOILED-Egg). Egan-Egg model named Brain Or Intestinal Estimated (BOILED) permeation predictive model (BOILED-Egg). The overall lecture of (Table 11) highlights that compounds L69 could be an excellent candidate as drugs. However, lead to further studies and manipulations. Ligand 65, Ligand 69 and their analogue compounds are not substrates of the renal organic cation transporter 2 (OCT2). The
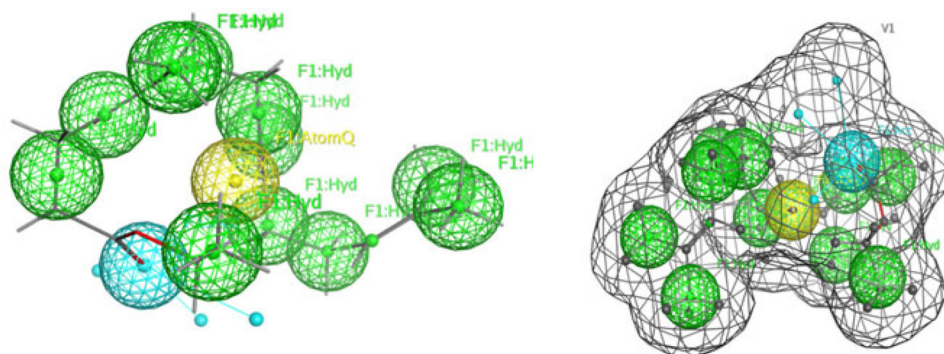
Figure 9. Pharmacophore Mapping of the E,E-Farnesyl acetate L69,Here,cyan color-hydrogen bond acceptor, link source and green color-hydrophobic.

Table 13. Energy balance of complexes formed with Superoxide Dismutase (SOD) under potent clinical antioxidant, some species of *Inula* genus and our results for essential oils of the *I.montana*.

Country	Score	Species	Major components	Reference
Some species of Inula genus				
Other experiments				
Bulgaria	−3.738	I. germanica	cis-Carvylacetate 20.7%	(Trendafilova et al., 2020)
	−3.265	I. bifrons	Muurola-4,10 (14) dien-1-ol 8.6%	
	−3.866	I. ensifolia	Hexanoicacid 8.1%	
		I. salicina	Hexanoicacid 8.3%	
Turkey	−3.135	I. graveolens	1,8-cineole 22.4%	(Kilic, 2014)
		I. oculus-christi	Bornylacetate 21.3%	
Algeria (Oran)	−3.601	I.viscosa	Bornylacetate 39.81%	(Boumaza, 2011)
France		I. graveolens	Bornylacetate 54%	
Italy (Sicily)	−3.674	I. crithmoides	Thymol 11.8%	(Fontana et al., 2014)
Tunisia	−3.450		p-Cymene 27.3%	(Jallali et al., 2014)
Italy			p-Cymene 30.1%	(Giamperi et al., 2010)
Spain			p-Cymene 53.8%	(Tsoukatou & Roussis, 1999)
Malta			p-Cymene 26.2%	
Greece	−3.142		ß-Phellandrene 30.7%	
Croatia (Badija Island)	−4.051	I. verbascifolia	Hexadecanoic acid 10.4%	(Giamperi et al., 2010)
Clinincal				
Acide Ascorbic	−3.329			
Ligand of reference				
Methionine *(Native)*	−3.388			
Ours Results				
E,E-Farnesyl acetateL69	−4.401	*Aerial parts of Inula Montana*		
E-Nerolidol acetate L65	−4.226			
Analog L65	−3.952	*Best analogue of compound L65 and L69 from* Aerial parts of *I.montana*		
Analog L69	−3.878			

absorption and distribution parameters, respectively, have been graphically represented by the extended and renewed version of the Edan-Egg model named Brain Or Intestinal Estimated (BOILED) permeation predictive model (BOILED-Egg (See Supplementary Materials Figure S5)

3.8. Pharmacokinetics and medicinal chemistry properties

The results Medicinal Chemistry and Pharmacokinetics revealed that all compounds have High GI absorptions. We notice that there was a complement between our results for assessment of ADME properties (Table9) and the predicted results in medicinal chemistry and pharmacokinetics (See Supplementary Materials Table S6).

E,E-Farnesyl acetate and E-Nerolidol acetate essential oils of *Aerial parts of I.montana* **(**Oxygenated sesquiterpenes). (Ligand 69) and Ligand 65) is predicted to be characterized

by a high lipophilicity and high coefficient of skin permeability logKp by providing Z-Nerolidol (Ligand 42), β-Acoradienol (Ligand 66) and α-Carinol (Ligand 56) (Oxygenated sesquiterpenes). We can explain that the more negative the logKp (with Kp in cm/s), the less the molecule is absorbed to the skin, which explains the reliability of our study. We cite the works which have valid the stability of complexes and their affinities by MOE software (Molecular Operating Environment (MOE), 2013; Mesli et al., 2013).

$$LogP_{o/w}L42 > LogP_{o/w}L65 > LogP_{o/w}L69.$$

So, Ligand L69 represents high affinity with Superoxide Dismutase (*SODs*) and ctDNA. Synthetic accessibility (SA) is a major factor to take into account in this selection process an acceptable value between 3.27, 3.43and 3.53 for the ligands (L69, L65 and L42) respectively, these are more encouraging compounds which can be synthesized or subjected to bioassays or other experiments. Our previous research has revealed that oils from our region have better biological

activities (Belabbes et al., 2017; Benyoucef et al., 2020). We cite the works which have valid the stability of complexes and their affinities by MOE software (Molecular Operating Environment (MOE), 2013; Mesli et al., 2013).

3.9. Pass (prediction of activity spectra for substances) and P450 site of metabolism (SOM) prediction

The predictions of activity spectra for substances (PASS prediction) study for best ligands were conducted to predict 10 intended biological activities. To carry out the PASS prediction experiment, Pa > 0.7 was kept, since this threshold give highly reliable prediction (Release, 2018). The PASS prediction results of all the best selected ligands are listed in Table 12. However, at Pa >0.7.

Prediction tests were also carried out for 10 biological activities, the results of which are in Table 12. We note that the compounds (E,E-Farnesyl acetate and E-Nerolidol acetate) shows some biological activities among the10 tested.

3.10. Pharmacophore mapping

The possible sites of metabolism by CYPs1A2, 2A6, 2B6, 2C19, 2C8, 2C9,2D6,2E1 and 3A4 of E,E Farnesylacetate L69 are summarized in (See Supplementary Materials Table S7). The possible sites of a chemical compound, where the metabolism by the isoforms of CYP 450 enzymes may be taking place, are illustrated by the circles on the chemical structure of the compound (Zaretzki et al., 2013).

The P450 SOM predictions showed that E,E-farnesyl acetate L69 had 4 sites of metabolism (SOMs)for the CYP450 1A2, 450 2B6 enzyme, CYP450 2C8, CYP450 2C9, CYP450 2C19 and 3 sites for CYP450 2A6.

The Pharmacophore Mapping is conveyed for the E,E-Farnesyl acetate L69 best *oral* ligand of the (Oxygenated sesquiterpenes) showed 1 hydrogen acceptor bonds,11 Hydrophobic groups and one Link source. It also generated a good number of good contacts with the Pharmacophore of (Superoxide Dismutase) (see Figure 9). The Pharmacophore of E,E-Farnesyl acetate generates a hypothesis which can be applied successfully in biological screening for further experiments (Dixon et al., 2006).

Validation of our results, for essential oils of the Aerial parts of *I.montana,* the synthetic antioxidant ascorbic acid and the methionine co-crystallized inhibitor and some species of *Inula* genus is mentioned in (Table 13).

Our molecular docking results with Superoxide Dismutase (SOD) coincide with clinical results; The Oxygenated sesquiterpenes compounds were the most dominant.

Ascorbic acid or vitamin C is involved in the main functions of the body: defense against viral and bacterial infections, protection of the wall of blood vessels, iron assimilation, antioxidant action (capture of free radicals), healing. The effect of ascorbate on the cell can be either protective or toxic. Epidemiological studies have shown that ascorbic acid sub-deficiencies can generate, in the long term, pathologies associated with oxidative stress. Research by (Jackson et al., 1998) has shown that normal extracellular

concentrations of ascorbic acid (30 to 150 micromoles/L) are not likely to prevent the interaction of NO (nitric oxide) with superoxide in physiological conditions.

Our ligands natural E,E-Farnesyl acetate L69 better stabilizes the system with its energy of Superoxide Dismutase $-4.401\,Kcal.mol^{-1}$ we compare with the components of Clinical Drugs (see Table 13). E,E-Farnesyl acetate could be an excellent candidate as drugs because represents better energy (See Supplementary Materials Table S3) for all ligand molecules and the volume of distribution (VDss) suggest that the drug will be distributed in plasma. And again from the (see table 5) E,E-Farnesyl acetate was characterized by a high lipophilicity and high coefficient of skin permeability LogKp. Therefore, we propose E,E-Farnesyl acetate as the best ligand which allows the inhibition of Superoxide Dismutase and ctDNA . And in the meantime, we suggest E,E-Farnesyl acetate present in (Oxygenated sesquiterpenes) with its validated activity Score (−4.401, −6.855) respectively for (Superoxide Dismutase and ctDNA) as a *new oral ligand*. The present bioinformatic analysis, molecular dynamics simulations used to scrutinize novel (Oxygenated sesquiterpenes). E,E-Farnesyl acetate inhibitor of enzyme (Superoxide Dismutase). Preceding studies have indicated that E,E-Farnesyl acetate has been shown to have antioxidant *activity*.

In vitro, many studies were focused on the inhibitory effect of the polyherbal compound (Bhāraṅgyādi), on key enzymes linked to investigate antioxidant activity, Superoxide Dismutase.

The result of (Kajaria et al., 2012) proved that polyherbal composed of three herbal drugs, namely (*Clerodendrum serratum*, *Hedychium spicatum* and *Inula racemosa)* formulation to be a good potential for antioxidant activity. The superoxide free radical showed a maximum scavenging activity of 62.45 ± 1.86 with EC_{50} 774.70 ± 5.45. Anti-lipidperoxidation free radicals showed a maximum absorption of 67.25 ± 1.89 with an EC50 of 700.08 ± 6.81. Ascorbic acid was used as standard with an IC_{50} value of 4.6 μg/ml. The mountain Inula is in the same family as the mountain arnica, Asteraceae. Mountain Arnica contains essential oils, thymol, sesquiterpene lactones and flavonoids. These plant molecules therefore act against inflammation through their ability to inhibit the production of prostaglandins. Extracts of A.montana flowers have a long history of use in European traditional medicine as a remedy to treat several ailments (Willuhn,1998), including pain, injuries, hematomas, dislocations, sprains, bruising, edema associated with fractures, rheumatic muscle and joint complaints, inflammations of the mucous membranes of the mouth and throat, furuncles, inflamed insect bites and surface phlebitis (Klaas et al., 2002). (Klaas et al., 2002) have proved that the inhibition of the transcription factor NFkB (underline the importance of Arnica preparations as anti-inflammatory remedies. (Morales Valverde et al., 2002) have proved that Inula Montana has an activity on the digestive system. (Haihaywanshi et al., 2017) have proved that Arnica montana also has anti-inflammatory and anti dandruff properties which assist its hair growth property.

In our research the software platform that integrates visualization, modeling and simulations (*MOE*) does not detect any mark of the hydrophobic interactions between E,E-Farnesyl acetate and both the Superoxide Dismutase; what may be connected to the large size of this compound and the high number of torsion angles. The results are identified to have inhibitory activities against novel Superoxide Dismutase. Of these ligands, E,E-Farnesyl acetate has a stronger bond and high absorption in the intestines with good bioavailability. Consequently, the study carried out in this research reveals many secrets conveyed by the use of magic plants. At the end of our study, we retain that all biological activity depends on the presence of certain metabolites inside the tissues of the plant. The results obtained in this study reveal that E,E-Farnesyl acetate and E-Nerolidol acetate have potential antioxidant ability in receptor (Superoxide Dismutase.) via ROS generation. Thus, E,E-Farnesyl acetate and E-Nerolidol acetate may be used for more analyses in order to further evaluate their efficiency in the reduction of oxidative stress and as a possible antioxidant to be used in the pharmaceutical industry.

4. Conclusion

The present research aimed at the chemical and biological investigation of the essential oil of the aerial part of the species *I. montana* belonging to the Asteraceae family in the hope of finding natural alternatives. Indeed, the chemical characterization of the essential oil revealed the predominance of oxygenated sesquiterpenes. On the other hand, the evaluation of antioxidant power has shown promising antioxidant activity, who could to be used as a natural food preservative and therefore as an alternative to synthetic chemicals. The inhibition of Superoxide Dismutase receptor was theoretically investigated by two methods of computational chemistry: molecular docking analyzes MD simulations, ADME properties and pharmacological knowledge. The results revealed that ligand natural inhibitor – E,E-Farnesyl acetate L69 and E-Nerolidol acetate L65 of (Essential oils from Aerial parts of *I.montana*) has an affinity to interact with cDNA and superoxidase. Although two compounds L65 and L69 have a potent binding affinity with Superoxide Dismutase in the docking simulation. Compound E,E-Farnesyl acetate showed better antioxidant, scavenging activity than other compounds. Molecular docking simulation and molecular dynamic (M.D) simulations indicated that the superior activity of compound E,E-Farnesyl acetate among other compounds might be attributed to the alkyl elongation at acetate chain. Moreover, the in silico assessment of the ADME properties and BOILED-Egg plot validate the compound 65 and 69 pass the brain barrier and have high lipophilicity and high coefficient of skin permeability in the intestines with good bioavailability. E,E-Farnesyl acetate (Oxygenated sesquiterpenes) has the highest binding affinity among all the inhibitors, it is proposed as a *natural orally active* drug and it may also be a good candidate for further biological and pharmacological investigations. All methods of computational have been able to identify promising oxygenated compounds that might represent future solutions in critical areas of human health. E,E-Farnesyl acetate Can be potential candidates for better performance. The docking results revealed that groove mechanism is followed by E,E-Farnesyl acetate to bind with DNA. The results of molecular docking provide useful information about drug-DNA interaction, which are valuable for the rational design of drugs as well as for understanding mechanism of these drugs at the molecular level. The results obtained in this study reveal that L65 and L69 has potent antioxidant ability in at least two receptors (Superoxide Dismutase and DNA sequence) via ROS generation. Thus, E,E-Farnesyl acetate and E-Nerolidol acetate may be used for more analyses in order to further evaluate their efficiency in the reduction of oxidative stress and as a possible antioxidant to be used in the pharmaceutical industry.

Ethics approval and consent to participate

Not applicable.

Consent for publication

Not applicable.

Disclosure statement

The authors declare no conflict of interest

ORCID

Nassim Djabou 🔵 http://orcid.org/0000-0002-6429-4082

Reference

Abu Saleh, M., Solayman, M., Hoque, M. M., Khan, M. A., Sarwar, M. G., & Halim, M. A. (2016). Inhibition of DNA topoisomerase type IIα (TOP2A) by mitoxantrone and its halogenated derivatives: A combined density functional and molecular docking study. *BioMed Research International*, *2016*, 6817502. https://doi.org/10.1155/2016/6817502

Adewole, L. O. (2002). Ageratum conyzoides L.(Asteraceae). *Fitoterapia*, *73*(1), 1–16.

Al-Mamary, M., Al-Meeri, A., & Al-Habori, M. (2002). Antioxidant activities and total phenolics of different types of honey. *Nutrition Research*, *22*(9), 1041–1047. https://doi.org/10.1016/S0271-5317(02)00406-2

Antonyuk, S., Strange, R. W., & Hasnain, S. S. (2010). Structural discovery of small molecule binding Sites in Cu-Zn human superoxide dismutase familial amyotrophic lateral sclerosis mutants provides insights for lead optimization. *Journal of Medicinal Chemistry*, *53*(3), 1402–1406. **doi:** https://doi.org/10.1021/jm9017948

Baser, K. H. C., & Buchbauer, G. (2010). *Essential oils science, technology, and applications*. CRC Press. https://doi.org/10.9781420063165-c3

Belabbes, R., Dib, M. E. A., Djabou, N., Ilias, F., Tabti, B., Costa, J., & Muselli, A. (2017). Chemical variability, antioxidant and antifungal activities of essential oils and hydrosol extract of Calendula arvensis L. from western Algeria. *Chemistry & Biodiversity*, 14(5), e1600482. https://doi.org/10.1002/cbdv.201600482

Benyoucef, F., Dib, M. E., Tabti, B., Zoheir, A., Costa, J., & Muselli, A. (2020). Synergistic effects of essential oils of Ammoides verticillata and satureja candidissima against many pathogenic microorganisms. *Anti-Infective Agents*, 18(1), 72–78. https://doi.org/10.2174/2211352517666190227161811

Bissantz, C., Kuhn, B., & Stahl, M. (2010). A medicinal chemist's guide to molecular interactions. *Journal of Medicinal Chemistry*, 53(14), 5061–5084. https://doi.org/10.1021/jm100112j

Boumaza, D. (2011). *Séparation et caractérisation chimique de quelques biomolécules actives de deux plantes médicinales: Inula viscosa, Rosmarinus officinalis de la région d'Oran* [Doctoral dissertation, Université d'Oran1-Ahmed Ben Bella].

Brünger, A., Brooks, C. L., III, & Karplus, M. (1984). Stochastic boundary conditions for molecular dynamics simulations of ST2 water. *Chemical Physics Letters*, 105(5), 495–500. https://doi.org/10.1016/0009-2614(84)80098-6

Chen, I. J., & Foloppe, N. (2008). Conformational sampling of druglike molecules with MOE and catalyst: Implications for pharmacophore modeling and virtual screening. *Journal of Chemical Information and Modeling*, 48(9), 1773–1791. https://doi.org/10.1021/ci800130k

Chenafa, H., Mesli, F., Daoud, I., Achiri, R., Ghalem, S., & Neghra, A. (2021). In silico design of enzyme α-amylase and α-glucosidase inhibitors using molecular docking, molecular dynamic, conceptual DFT investigation and pharmacophore modelling. *Journal of Biomolecular Structure and Dynamics*, 39, 1–22. https://doi.org/10.1080/07391102.2021.1882340

Cheng, F., Li, W., Zhou, Y., Shen, J., Wu, Z., Liu, G., Lee, P. W. Tang, Y. (2012). admetSAR: A comprehensive source and free tool for assessment of chemical ADMET properties. *Journal of Chemical Information and Modeling*, 52(11). https://doi.org/10.1021/ci300367a

Clément, G., & Slenzka, K. (Eds.). (2006). *Fundamentals of space biology: Research on cells, animals, and plants in space* (Vol. 18). Springer Science & Business Media.

Cross, J. B., Thompson, D. C., Rai, B. K., Baber, J. C., Fan, K. Y., Hu, Y., & Humblet, C. (2009). Comparison of several molecular docking programs: Pose prediction and virtual screening accuracy. *Journal of Chemical Information and Modeling*, 49(6), 1455–1474. https://doi.org/10.1021/ci900056c

Dal Ben, D., Buccioni, M., Lambertucci, C., Thomas, A., & Volpini, R. (2013). Simulation and comparative analysis of binding modes of nucleoside and non-nucleoside agonists at the A2B adenosine receptor. *In Silico Pharmacology*, 1(1), 24. 4 https://doi.org/10.1186/2193-9616-1-24

Daoud, I., Melkemi, N., Salah, T., & Ghalem, S. (2018). Combined QSAR, molecular docking and molecular dynamics study on new Acetylcholinesterase and Butyrylcholinesterase inhibitors. *Computational Biology and Chemistry*, 74, 304–326. https://doi.org/10.1016/j.compbiolchem.2018.03.021

Didierjean, C., & Tête-Favier, F. (2016). Introduction to Protein Science. Architecture, Function and Genomics. By Arthur M. Lesk. Oxford University Press, 2016. Pp. 466. Paperback. Price GBP 39.99. ISBN 9780198716846. *Acta Crystallographica Section D Structural Biology*, 72(12), 1308–1309. https://doi.org/10.1107/S2059798316018283

Dixon, S. L., Smondyrev, A. M., Knoll, E. H., Rao, S. N., Shaw, D. E., & Friesner, R. A. (2006). PHASE: A new engine for pharmacophore perception, 3D QSAR model development, and 3D database screening: 1. Methodology and preliminary results. *Journal of Computer-Aided Molecular Design*, 20(10-11), 647–671. https://doi.org/10.1007/s10822-006-9087-6

Djabou, N., Lorenzi, V., Guinoiseau, E., Andreani, S., Giuliani, M.-C., Desjobert, J.-M., Bolla, J.-M., Costa, J., Berti, L., Luciani, A., & Muselli, A. (2013). Phytochemical composition of Corsican Teucrium essential oils and antibacterial activity against foodborne or toxi-infectious pathogens. *Food Control.*, 30(1), 354–363. https://doi.org/10.1016/j.foodcont.2012.06.025

Drew, H. R., Wing, R. M., Takano, T., Broka, C., Tanaka, S., Itakura, K., & Dickerson, R. E. (1981). Structure of a B-DNA dodecamer: Conformation and dynamics. *Proceedings of the National Academy of Sciences of the United States of America*, 78(4), 2179–2183. **doi:** https://doi.org/10.1073/pnas.78.4.2179

El Omari, N., Sayah, K., Fettach, S., El Blidi, O., Bouyahya, A., Faouzi, M. E. A., Kamal, R., & Barkiyou, M. (2019). Evaluation of in vitro antioxidant and antidiabetic activities of Aristolochia longa extracts. *Evidence-Based Complementary and Alternative Medicine : eCAM*, 2019, 7384735. https://doi.org/10.1155/2019/7384735

Filimonov, D. A., Lagunin, A. A., Gloriozova, T. A., Rudik, A. V., Druzhilovskii, D. S., Pogodin, P. V., & Poroikov, V. V. (2014). Prediction of the biological activity spectra of organic compounds using the PASS online web resource. *Chemistry of Heterocyclic Compounds*, 50(3), 444–457. https://doi.org/10.1007/s10593-014-1496-1

Fontana, G., Bruno, M., Senatore, F., & Formisano, C. (2014). Volatile constituents of aerial parts of two Mediterranean species of Inula: Inula crithmoides L. and I. verbascifolia (Willd.) Hausskn. (Asteraceae)). *Natural Product Research*, 28(13), 984–993. https://doi.org/10.1080/14786419.2014.902821

Fouzia, M., Noureddine, M., Amina, G., & Said, G. (2018). Comparative study of aromatase enzyme inhibition by synthetic and natural ligand: Molecular modeling and conceptual DFT investigation. *Current Enzyme Inhibition*, 14(2), 104–113. https://doi.org/10.2174/1573408014666180222135450

Fouzia, M., & Salim, B. (2019). Virtual screening of natural and synthetic inhibitors of cyclooxygenase COX-2 enzyme using docking-scoring functions. *Journal of Applied Pharmaceutical Science*, 9(01), 020–027.

Geronikaki, A., Poroikov, V., Hadjipavlou-Litina, D., Filimonov, D., Lagunin, A., & Mgonzo, R. (1999). Computer aided predicting the biological activity spectra and experimental testing of new thiazole derivatives. *Quantitive Structure-Activity Relationships*, 18(1), 16–25. https://doi.org/10.1002/(sici)1521-3838(199901)18:1<16::aid-qsar16>3.0.co;2-o

Giamperi, L., Bucchini, A., Fraternale, D., Genovese, S., Curini, M., & Ricci, D. (2010). Composition and antioxidant activity of Inula crithmoides essential oil grown in central Italy (Marche region). *Natural Product Communications*, 5(2), 315–318. https://doi.org/10.1177/1934578X1000500230

Haihaywanshi, M. S., Gouri, T., Gupta, A., & Jain, S. (2017). Arnica hydrogel: An oil replacement for hair loss treatment. *Journal of Drug Delivery and Therapeutics*, 7(7), 23–25.

Halgren, T. A. (1996). Merck molecular force field. I. Basis, form, scope, parameterization, and performance of MMFF94. *Journal of Computational Chemistry*, 17(5-6), 490–519. https://doi.org/10.1002/(SICI)1096-987X(199604)17:5/6<490::AID-JCC1>3.0.CO;2-P

Halgren, T. A. (1999). MMFF VII. Characterization of MMFF94, MMFF94s, and other widely available force fields for conformational energies and for intermolecular-interaction energies and geometries. *Journal of Computational Chemistry*, 20(7), 730–748. https://doi.org/10.1002/(SICI)1096-987X(199905)20:7<730::AID-JCC8>3.0.CO;2-T

Halliwell, B. (1995). Antioxidant characterization: Methodology and mechanism. *Biochemical Pharmacology*, 49(10), 1341–1348. https://doi.org/10.1016/0006-2952(95)00088-H

Huai, J., & Zhang, Z. (2019). Structural properties and interaction partners of familial ALS-associated SOD1 mutants. *Frontiers in Neurology*, 10, 527. https://doi.org/10.3389/fneur.2019.00527

Ischiropoulos, H., Zhu, L., Chen, J., Tsai, M., Martin, J. C., Smith, C. D., & Beckman, J. S. (1992). Peroxynitrite-mediated tyrosine nitration catalyzed by superoxide dismutase. *Archives of Biochemistry and Biophysics*, 298(2), 431–437. https://doi.org/10.1016/0003-9861(92)90431-u

Jackson, T. S., Xu, A., Vita, J. A., & Keaney, J. F. Jr, (1998). Ascorbate prevents the interaction of superoxide and nitric oxide only at very high physiological concentrations. *Circulation Research*, 83(9), 916–922. https://doi.org/10.1161/01.res.83.9.916

Jallali, I., Zaouali, Y., Missaoui, I., Smeoui, A., Abdelly, C., & Ksouri, R. (2014). Variability of antioxidant and antibacterial effects of essential oils and acetonic extracts of two edible halophytes: Crithmum

maritimum L. and Inula crithmoïdes L. *Food Chemistry*, 145, 1031–1038. https://doi.org/10.1016/j.foodchem.2013.09.034

Jennings, W., & Shibamoto, T. (1980). Analytical considerations. In H. B., Jovanovich (Ed.), *Qualitative analysis of flavour and fragrance volatiles by glass-capillary gas chromatography* (1st ed., pp. 1–27). Academic Press.

Jorgensen, W. L., Maxwell, D. S., & Tirado-Rives, J. (1996). Development and testing of the OPLS all-atom force field on conformational energetics and properties of organic liquids. *Journal of the American Chemical Society*, 118(45), 11225–11236. https://doi.org/10.1021/ja9621760

Kabouche, Z. (2014). Etude phytochimique et biologique des espèces Biscutella raphanifolia, Zilla macroptera, Inula graveolens et Inula viscosa.

Kajaria, D. K., Gangwar, M., Sharma, A. K., Tripathi, Y. B., Tripathi, J. S., & Tiwari, S. (2012). Evaluation of in vitro antioxidant capacity and reducing potential of polyherbal drug- Bhāraṅgyādi. *Ancient Science of Life*, 32(1), 24–28. https://doi.org/10.4103/0257-7941.113798

Kilic¸, O. (2014). Chemical composition of two Inula sp.(Asteraceae) species from Turkey. *Iğdır Üniversitesi Fen Bilimleri Enstitüsü Dergisi*, 4(1), 15–19.

Klaas, C. A., Wagner, G., Laufer, S., Sosa, S., Della Loggia, R., Bomme, U., Pahl, H. L., & Merfort, I. (2002). Studies on the anti-inflammatory activity of phytopharmaceuticals prepared from Arnica flowers. *Planta Medica*, 68(5), 385–391. https://doi.org/10.1055/s-2002-32067

Law, V., Knox, C., Djoumbou, Y., Jewison, T., Guo, A. C., Liu, Y., Maciejewski, A., Arndt, D., Wilson, M., Neveu, V., Tang, A., Gabriel, G., Ly, C., Adamjee, S., Dame, Z. T., Han, B., Zhou, Y., & Wishart, D. S. (2014). DrugBank 4.0: Shedding new light on drug metabolism. *Nucleic Acids Research*, 42(Database issue), D1091–D1097. https://doi.org/10.1093/nar/gkt1068

Lipinski, C. A., Lombardo, F., Dominy, B. W., & Feeney, P. J. (1997). Experimental and computational approaches to estimate solubility and permeability in drug discovery and development settings. *Advanced Drug Delivery Reviews*, 23(1-3), 3–25. https://doi.org/10.1016/j.addr.2012.09.019

Lishchynskyi, A., Novikov, M. A., Martin, E., Escudero-Adán, E. C., Novák, P., & Grushin, V. V. (2013). Trifluoromethylation of aryl and heteroaryl halides with fluoroform-derived CuCF3: Scope, limitations, and mechanistic features. *The Journal of Organic Chemistry*, 78(22), 11126–11146. https://doi.org/10.1021/jo401423h

Marikovsky, M., Ziv, V., Nevo, N., Harris-Cerruti, C., & Mahler, O. (2003). Cu/Zn superoxide dismutase plays important role in immune response. *Journal of Immunology (Baltimore, Md. : 1950)*, 170(6), 2993–3001. https://doi.org/10.4049/jimmunol.170.6.2993

McClinton, M. A., & McClinton, D. A. (1992). Trifluoromethylations and related reactions in organic chemistry. *Tetrahedron*, 48(32), 6555–6666. https://doi.org/10.1016/S0040-4020(01)80011-9

Mesli, F., Medjahed, K., & Ghalem, S. (2013). Prediction of structural and thermodynamic properties of three products: 1-bromobenzene, tetrachlorethylene and 4-hydroxy-chromen-2-one using numerical methods. *Research on Chemical Intermediates*, 39(4), 1877–1895. https://doi.org/10.1007/s11164-012-0722-7

Molecular Operating Environment (MOE) (2013). 08 *Chemical Computing Group Inc.*, 1010 Sherbooke St. West, Suite #910,. Montreal, QC, Canada, H3A 2R7, 2019.

Morales Valverde, R., Tardío, J., & Pascual, H. (2002). *Alimentos silvestres de Madrid: Guía de plantas y setas de uso alimentario tradicional en la Comunidad de Madrid*. Comunidad Autónoma. .

Nadia, B., Mesli, F., Zahra, B. F., Merad-Boussalah, N., Radja, A., Muselli, A., … Dib, M. E. A. (2020). Chemical composition variability and vascular endothelial growth factor receptors inhibitory activity of Inulaviscosa essential oils from Algeria. *Journal of Biomolecular Structure and Dynamics*, 39, 1–19.

Nair, H. K., Seravalli, J., Arbuckle, T., & Quinn, D. M. (1994). Molecular recognition in acetylcholinesterase catalysis: Free-energy correlations for substrate turnover and inhibition by trifluoro ketone transition-state analogs. *Biochemistry*, 33(28), 8566–8576. https://doi.org/10.1021/bi00194a023

Nalini, C. N., Deepthi, S. R., Ramalakshmi, N., & Uma, G. (2011). Toxicity risk assesment of isatins. *Rasayan Journal of Chemistry.*, 4(4), 829–833.

National Institute of Standards and Technology (1999). NIST/EPA/NIH Mass Spectral Library. PC Version 1.7.

Navidpour, L., Shadnia, H., Shafaroodi, H., Amini, M., Dehpour, A. R., & Shafiee, A. (2007). Design, synthesis, and biological evaluation of substituted 2-alkylthio-1,5-diarylimidazoles as selective COX-2 inhibitors . *Bioorganic & Medicinal Chemistry*, 15(5), 1976–1982. https://doi.org/10.1016/j.bmc.2006.12.041

Neidle, S. (2001). DNA minor-groove recognition by small molecules. *Natural Product Reports*, 18(3), 291–309. https://doi.org/10.1039/a705982e

Nisha, C. M., Kumar, A., Nair, P., Gupta, N., Silakari, C., Tripathi, T., & Kumar, A. (2016). Molecular docking and in silico ADMET study reveals acylguanidine 7a as a potential inhibitor of β-secretase. *Advances in Bioinformatics*, 2016, 1–6. https://doi.org/10.1155/2016/9258578

Oury, T. D., Day, B. J., & Crapo, J. D. (1996). Extracellular superoxide dismutase: A regulator of nitric oxide bioavailability. *Laboratory Investigation; a Journal of Technical Methods and Pathology*, 75(5), 617–636.

Oyaizu, M. (1986). Studies on product of browning reaction prepared from glucose amine. *The Japanese Journal of Nutrition and Dietetics*, 44(6), 307–315. https://doi.org/10.5264/eiyogakuzashi.44.307

Parr, R. G. (1989). W. Yang Density functional theory of atoms and molecules. *Oxford University Press*, 1, 989.

Pascual, H., & Morales, R. (2002). *Alimentos silvestres de Madrid*. La Librería.

Patel, M., Chilton, M. L., Sartini, A., Gibson, L., Barber, C., Covey-Crump, L., Przybylak, K. R., Cronin, M. T. D., & Madden, J. C. (2018). Assessment and reproducibility of quantitative structure–activity relationship models by the nonexpert. *Journal of Chemical Information and Modeling*, 58(3), 673–682. https://doi.org/10.1021/acs.jcim.7b00523

Plano, D., Karelia, D. N., Pandey, M. K., Spallholz, J. E., Amin, S., & Sharma, A. K. (2016). Design, synthesis, and biological evaluation of novel selenium (Se-NSAID) molecules as anticancer agents. *Journal of Medicinal Chemistry*, 59(5), 1946–1959. https://doi.org/10.1021/acs.jmedchem.5b01503

Release, S. (2018). *2: Maestro, version 11.8*. Schrödinger, LLC.

Sarwar, M. G., Ajami, D., Theodorakopoulos, G., Petsalakis, I. D., & Rebek, J. (2013). Amplified halogen bonding in a small space. *Journal of the American Chemical Society*, 135(37), 13672–13675. https://doi.org/10.1021/ja407815t

Sarwar, M. G., Dragisic, B., Salsberg, L. J., Gouliaras, C., & Taylor, M. S. (2010). Thermodynamics of halogen bonding in solution: Substituent, structural, and solvent effects. *Journal of the American Chemical Society*, 132(5), 1646–1653. https://doi.org/10.1021/ja9086352

Semaoui, M., Mesli, F., Dib, M. E. A., Tabti, B., Achiri, R., Costa, J., & Muselli, A. (2020). Statistical analysis/theoretical investigations of novel vascular endothelial growth factor of Davanoide from Scolymus grandifloras Desf as potent anti-angiogenic drug properties. *Journal of Biomolecular Structure and Dynamics*, 39, 1–20. https://doi.org/10.1080/07391102.2020.1851301

Singh, D., Gawande, D. Y., Singh, T., Poroikov, V., & Goel, R. K. (2014). Revealing pharmacodynamics of medicinal plants using in silico approach: A case study with wet lab validation. *Computers in Biology and Medicine*, 47, 1–6. https://doi.org/10.1016/j.compbiomed.2014.01.003

Stewart, J. J. (2007). Optimization of parameters for semiempirical methods V: Modification of NDDO approximations and application to 70 elements. *Journal of Molecular Modeling*, 13(12), 1173–1213. https://doi.org/10.1007/s00894-007-0233-4

Suthakaran, R., Kavimani, S., Venkapayya, P., & Suganthi, K. (2008). Synthesis and antimicrobial activity of 3-(2-(4z)-4-substituted benzylidene-4, 5-dihydro-5-oxo-2-phenyl imidazol-1-yl) ethyl)-6, 8-un/dibromo substituted-2-substituted quinazoline-(3H)-one. *Rasayan Journal of Chemistry*, 1(1), 22–29.

Toda, M., Kubo, R., Saitō, N., & Hashitsume, N. (1991). *Statistical physics II: nonequilibrium statistical mechanics* (Vol. 2). Springer Science & Business Media.

Trendafilova, A., Todorova, M., Ozek, T., Ozek, G., & Aneva, I. (2020). Volatile constituents of four Inula species of Bulgarian origin. *Biochemical Systematics and Ecology*, 90, 104035. https://doi.org/10.1016/j.bse.2020.104035

Tsoukatou, M., & Roussis, V. (1999). Chemical composition and intra Mediterranean variation of the Inula crithmoides L. oil. *Journal of Essential Oil Research*, *11*(2), 199–202. https://doi.org/10.1080/10412905.1999.9701110

Wang, X., Shen, Y., Wang, S., Li, S., Zhang, W., Liu, X., Lai, L., Pei, J., & Li, H. (2017). PharmMapper 2017 update: A web server for potential drug target identification with a comprehensive target pharmacophore database. *Nucleic Acids Research*, *45*(W1), W356–W360. https://doi.org/10.1093/nar/gkx374

Wang, W., & Skeel, R. D. (2003). Analysis of a few numerical integration methods for the Langevin equation. *Molecular Physics*, *101*(14), 2149–2156. https://doi.org/10.1080/0026897031000135825

Wichi, H. P. (1988). Enhanced tumor development of butylated hydroxyanisol (BHA) from the prospective of effect on fore stomach and oesophageal squamous epithlium. *Food and Chemical Toxicology.*, *26*, 717–723.

Willuhn, G. (1998). Arnica flowers: Pharmacology, toxicolgy, and analysis of the sesquiterpene lactones—Their main active substances. *Phytomedicines of Europe, 691*, 118-132. https://doi.org/10.1021/bk-1998-0691.ch010

Yang, H., Sun, L., Li, W., Liu, G., & Tang, Y. (2018). In silico prediction of chemical toxicity for drug design using machine learning methods and structural alerts. *Frontiers in Chemistry*, *6*, 30. https://doi.org/10.3389/fchem.2018.00030

Zaretzki, J., Bergeron, C., Huang, T. W., Rydberg, P., Swamidass, S. J., & Breneman, C. M. (2013). RS-WebPredictor: A server for predicting CYP-mediated sites of metabolism on drug-like molecules. *Bioinformatics (Oxford, England)*, *29*(4), 497–498. https://doi.org/10.1093/bioinformatics/bts705